Journal of Hydrology: Regional Studies 35 (2021) 100828

Contents lists available at ScienceDirect

Journal of Hydrology: Regional Studies

journal homepage: www.elsevier.com/locate/ejrh

Impacts of climate and environmental changes on water resources: A multi-scale study based on Nakanbé nested watersheds in West African Sahel

Y. Patrick Gbohoui [a,b,*], Jean-Emmanuel Paturel [b], Fowe Tazen [a], Lawani A. Mounirou [a], Roland Yonaba [a], Harouna Karambiri [a], Hamma Yacouba [a]

[a] Laboratoire Eaux, HydroSystèmes et Agriculture (LEHSA), Institut International d'Ingénierie de l'Eau et de l'Environnement (2iE), Rue de la Science, Ouagadougou 01 01-BP-594, Burkina Faso[1]

[b] HydroSciences Montpellier, Univ Montpellier, CNRS, IRD, 163 rue Auguste Broussonnet, 34090, Montpellier, France

ARTICLE INFO

Keywords:
Climate change
Environmental change
Climate-environment interaction
Budyko framework
Sahelian hydrological paradox
Nakanbé River watershed

ABSTRACT

Study region: Nakanbé River watershed in the West Africa Sahel (WAS).
Study focus: This study aims to better understand the hydrological behavior of WAS watersheds, which experienced Sahelian hydrological paradoxes (SHP). Budyko framework was employed to evaluate the impact of climate change, environmental change and climate-environment interaction on surface runoff change in seven nested watersheds (38 – 21,178 km^2) over the period 1965–2018.
New hydrological insights for the region: Based on time-series stationarity statistical tests, the study period was divided into one baseline period (1965–1977) and three impacted periods (1978−1994, 1995−2006 and 2007−2018). Compared to the baseline period, the period 1978−1994 was characterized by a decrease in precipitation and an increase in runoff (first SHP). During the period 1995–2018, the runoff coefficient, which increased despite the observed re-greening, was interpreted as evidence of the second SHP. The impact study showed that environmental change was the main driver of the first SHP (contribution reached +175 %), then climate-environment interaction became increasingly dominant during the second SHP (contribution reaching +68 %). The watersheds evolution in Budyko framework showed that the Fu Budyko-type model parameter appears to be a good indicator of soil water holding capacity spatio-temporal variability. Our results highlight the consequences of climate and environmental changes on surface runoff in the Sahelian context and might help in developing informed land management and restoration strategies to control runoff coefficients.

1. Introduction

Climate change (CC) and environmental change (EC) affect the hydrological behavior of most rivers watersheds in the world (Bai et al., 2019; Descroix et al., 2018; Grijsen et al., 2013; Kang et al., 2020; Karambiri et al., 2011; Mango et al., 2011; Piemontese et al.,

* Corresponding author at: Laboratoire Eaux, HydroSystèmes et Agriculture (LEHSA), Institut International d'Ingénierie de l'Eau et de l'Environnement (2iE), Rue de la Science, Ouagadougou 01 01-BP-594, Burkina Faso.
E-mail addresses: patrickgbohoui@gmail.com (Y.P. Gbohoui), jean-emmanuel.paturel@ird.fr (J.-E. Paturel).
[1] 2ie@2ie-edu.org.

https://doi.org/10.1016/j.ejrh.2021.100828
Received 5 November 2020; Received in revised form 27 April 2021; Accepted 30 April 2021
Available online 10 May 2021

2019; Svensson et al., 2005). At the watershed scale, EC includes changes in land use and land cover (LULC) and soil physical properties. Thus, the hydrological cycle of the watersheds has undergone profound modifications. Floods have become increasingly devastating and water resources threatened (Descroix et al., 2018, 2009; Kundzewicz et al., 2005; Mangini et al., 2018; Nka et al., 2015; Paturel et al., 2003; Robson, 2002; Svensson et al., 2005). Given such drastic changes, a better understanding of watersheds hydrological behavior is critical to implement effective measures for surface runoff regulation, or at least, to strengthen resilience. The studies examining the impacts of CC and EC on water resources have been often used to investigate the hydrological behavior of watersheds (Dooge, 1992; Kang et al., 2020; Mango et al., 2011; Pellarin et al., 2013; Piemontese et al., 2019; Taylor et al., 2011; Zhang et al., 2019). According to Blöschl et al. (2007) and Sivapalan et al. (2003), the methods used to assess CC and EC impacts on water resources can be summarized into upward and downward approaches.

The so-called *upward* approach starts with a thorough understanding of physical processes to further set up a detailed hydrological model based on conservation equations (Blöschl et al., 2013). This approach requires a long time series of climate and environmental data. In addition, the detailed models are multi-parametric, which might lead to an increase in uncertainties in the results, hence an overall increased difficulty in analyzing the outputs in a given study context (Blöschl et al., 2007). The so-called *downward* approach seeks to explain the behavior of the hydrological system as a whole. It consists of analyzing the evolution of hydrological response to come up with hypotheses, which explain the mechanisms and conditions underlying the observed trends (Harman and Troch, 2014). The downward approach includes statistical/empirical methods (linear regression, machine learning), conceptual frameworks (Budyko, Tomer-Schilling) and analytical methods (Arora, 2002; Budyko, 1974; Guo et al., 2019; Peng et al., 2013; Tomer and Schilling, 2009; Zuo et al., 2014; Zhu et al., 2019; Zhang et al., 2017). In this set, the Budyko framework (Budyko, 1974) is widely used for impact studies in hydrology through parametric models. Such models do not require environmental data; however, the signatures of environmental dynamics are captured through the evolution of actual evapotranspiration (AE), defined as a function of potential evapotranspiration (PE) and precipitation (P) (Budyko, 1974; Sposito, 2017). Climate elasticity and decomposition of the Budyko curve are the two techniques used to quantify the impacts.

The climate elasticity-based method quantifies the impact of CC on water resources and the remainder is attributed to non-climatic factors (Arora, 2002). The Budyko curve decomposition is a conceptual method that partitions runoff change into impacts of CC and human interference (Wang and Hejazi, 2011), which assumes that runoff change is solely due to CC and human interference. However, the interaction between climate and environment is recognized at all spatio-temporal scales (Dearing, 2006; Diello, 2007; Gao et al., 2014). Therefore, it is essential to isolate the impact of CC, EC and climate-environment interaction on water resources.

In the Budyko-type model, the impact of human interferences is quantified through a parameter largely controlled by environmental variables (Li et al., 2013). Several studies have shown that the value of the Budyko parameter is a function of the proportion of the watershed covered by vegetation (Ning et al., 2019; Teuling et al., 2019; Zhang et al., 2004, 2001, 1999), but the relationships established were not stable and varied across studies (Donohue et al., 2011; Jiang et al., 2015; Li et al., 2013; Liu et al., 2019; Ning et al., 2019; Wang and Tang, 2014; Zhang et al., 2004, 2019a).

Among the several studies applying the Budyko framework to assess the contributions of CC and EC to surface runoff change, only Li et al. (2013) took into account the Niger River watershed in West African Sahel (WAS). Most of the impact studies carried in the WAS have been limited to assessing the effects of CC (Grijsen et al., 2013; Karambiri et al., 2011). A few studies gave an interest in the effects of EC but were limited to qualitative assessments (Nka et al., 2015) or based on upward approaches through hydrological modeling (Gal et al., 2017; Yonaba et al., 2021). However, the scarcity and the low quality of data that characterize Africa (Hasan et al., 2018; Mahé, 2006) severely hamper the application of such upward approaches (Blöschl et al., 2007). The WAS is known for the fragility of its hydrological system, for which a wide range of questions remains unanswered. Since 1950, the climate in this zone has been characterized by i) a continuous increase in potential evapotranspiration (PE) due to global warming; ii) a wet period (1950–1970), followed by a drought period (1970–1990) and recovery of precipitation since the 1990s (De Longueville et al., 2016; Lebel and Ali, 2009; Mahé, 2006). Since the 1980s drought, the hydrological behavior of some hydro-systems has become paradoxical (Descroix et al., 2018; Mahé and Paturel, 2009; Wendling et al., 2019). The first Sahelian hydrological paradox (SHP), characterized by an exacerbated increase in runoff, occurred during the drought. The second SHP, characterized by an increase in the runoff coefficient despite the general re-greening of the WAS, has been observed since the precipitation recovery (Descroix et al., 2018). These SHPs fostered flooding, overflowing in hydraulic infrastructures, erosion and land degradation.

The Nakanbé River is an important tributary of the Volta River in West Africa. It takes its source from the Sahelian zone in Burkina Faso and it is one of the main freshwater resources of the country (Ibrahim, 2012). A significant part of its drainage area (Nakanbé at Wayen) is located in the WAS and has also been experiencing changes in the hydrologic regimes (Diello, 2007; Mahé et al., 2005; Paturel et al., 2017). The overflow of the large Bagré dam (downstream of Wayen station) in 1994, two years after its impoundment, is such an example (Mahé et al., 2005; Paturel et al., 2003). Therefore, the Nakanbé watershed is an interesting case study to shed light on the evolution of the WAS watersheds hydrological behavior by assessing the isolated and combined impacts of CC and EC on surface runoff change.

The objectives of this study were: i) to quantify the contributions of CC, EC and climate-environment interaction to surface runoff change across seven nested watersheds; ii) to investigate the relationship between Budyko model parameter and the vegetation coverage.

2. Study area and data

2.1. Study area

The study area (Fig. 1) lies in the Sahel characterized by a short wet season (June-October), higher variability in precipitation, high evapotranspiration rates and significant thermal amplitudes. The average annual precipitation varies between 200 mm and 1200 mm and potential evapotranspiration ranges between 1500 and 3000 mm per year. The Nakanbé River is an important tributary of the trans-boundary Volta River shared by Benin, Burkina Faso, Ivory Coast, Ghana, Mali and Togo. The Nakanbé River watershed in Burkina Faso covers about 15 % of the country with high population density and shelters more than 50 % of its water reservoirs (Ibrahim, 2012). The watershed relief is generally flat with altitudes varying between 259 and 526 m. The crystalline basement, which occupies the underground watershed, is not favorable to a significant mobilization of groundwater resources. Upstream Wayen gauging station, several natural and artificial reservoirs can be found in the Nakanbé watershed, the most important of which are the Bam Lake (41 million m^3), the Dourou dam (100 million m^3) and Ziga dam (200 million m^3) impounded in 1995 and 2000 respectively (Fig. 1). The Ziga dam is mainly used for water supply to Ouagadougou (the capital city of Burkina Faso) and the Dourou dam is mainly used for agricultural purposes. In the Nakanbé watershed, LULC changes were significant over the period 1972–1992, but have become stable since 1992 (Diello, 2007).

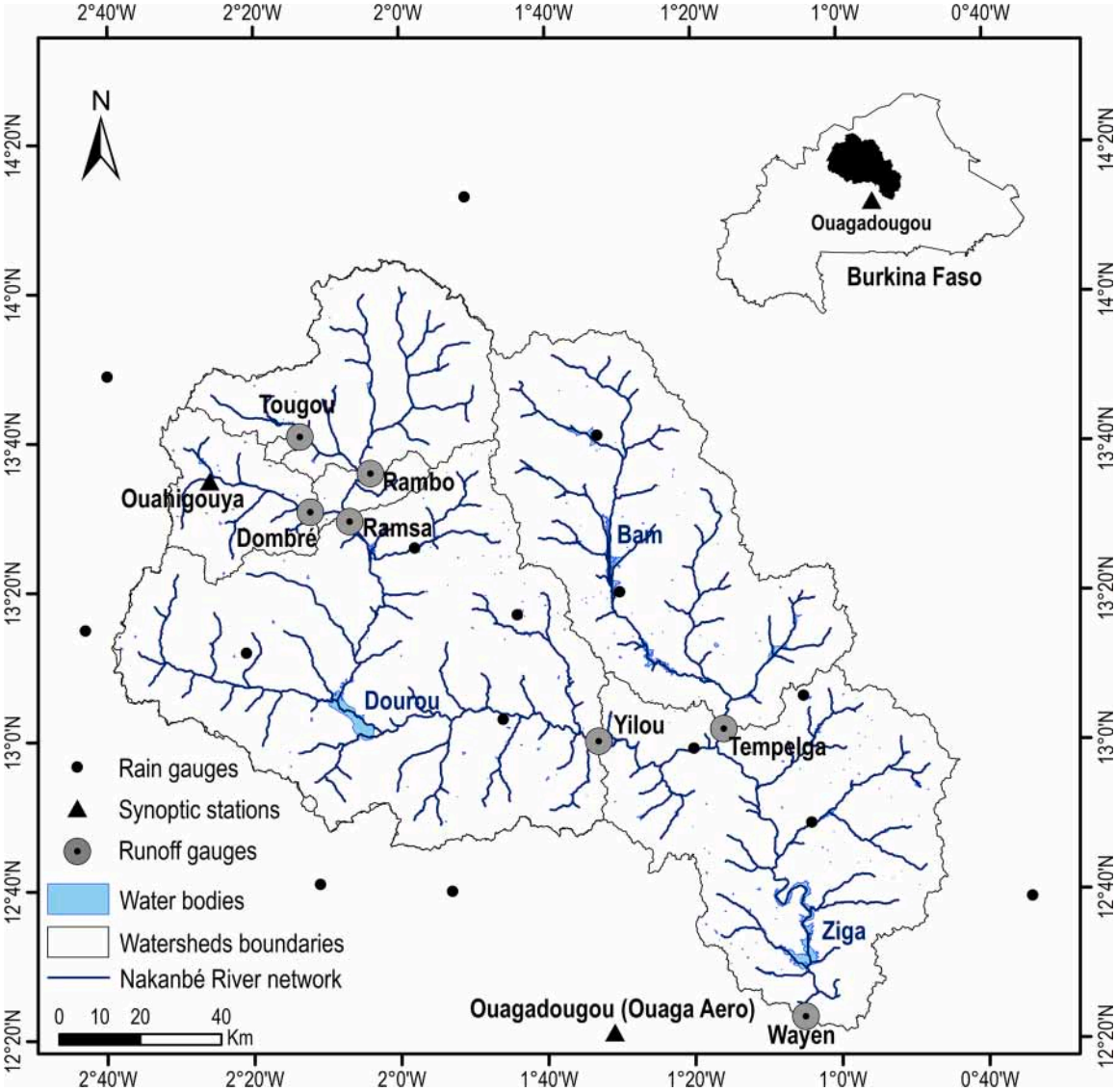

Fig. 1. The Nakanbé nested watersheds at Wayen (38 - 21,178 km^2), located in the West Africa Sahel, with drainage network, water bodies, available rain gauges, synoptic stations and runoff gauges.

2.2. Hydro-climatic data

Hydro-climatic data used in this study included precipitation (P), potential evapotranspiration (PE), actual evapotranspiration (AE) and surface runoff (R). Fig. 2 shows the flowchart used for data processing. In general, the quality control of the observed data collected consisted of an exploratory analysis to detect outliers and gaps. Some additional checks specific to each type of data were also carried out. At the end of data quality control, the valid observations were used to identify the appropriate databases to fill in the gaps after bias-correction, if necessary.

Hydrological data concerned the daily discharges over the period 1965–2018 at seven gauging stations in the Nakanbé River watershed (presented in Fig. 1), six of which were provided by the hydrological services ("Direction Générale des Ressources en Eau, DGRE") in Burkina-Faso. The daily data from the Tougou watershed gauging station was provided by 2iE Institute for the period 2004−2018. As shown in Fig. 3, these data have several gaps. In this study, it has been assumed that a valid year is a year without missing data during the wet season (June-October). Furthermore, when the river cross-section at the gauging station underwent significant changes without updating its rating curve, all data measured after the modification were declared missing. Thus, three gauging stations (Wayen, Ramsa and Rambo) had valid data for more than 20 years (Fig. 3). Annual runoffs at Wayen station after the construction of Ziga and Dourou dams (from 1995) were reconstructed based on monitoring data obtained from DGRE and water withdrawals monitoring from the water and sanitation services ("Office National de l'Eau et de l'Assainissement, ONEA") in Burkina Faso.

The daily time series of P and PE came from the SIEREM database (Boyer et al., 2006) and the national meteorological services ("Agence Nationale de la Météorologie, ANAM") in Burkina Faso (Table 1). These included data from seventeen stations (among which two are synoptic stations), as shown in Fig. 1. The meteorological data collected covers the period 1965−2015, but most of them ended in 2000 (Fig. 3). To fill the gaps, the databases ARC.2, CHIRPSv2.0, MSWEPv2.2, TerraClimate and CRU TS v 4.03 (see Table 1 for details) were identified. The two synoptic stations (OuagaAero and Ouahigouya) with complete data from 1965 to 2015 were used to select the most suitable databases for the Nakanbé watershed.

For the precipitation time series, three databases (ARC v2, CHIRPS v2.0 and MSWEP v2.2) were compared to observations (at synoptic stations) over the period 2000-2015 as it contained 90 % of the gaps. The Kling-Gupta Efficiency (KGE) performance criterion (Gupta et al., 2009) and the Percent Bias, PBIAS (Moriasi et al., 2007) were applied to assess database performance. The ARC v2 database was finally selected as it presented the best performance overall (KGE $>$ 0.8 and PBIAS $<$ 2.6). Similarly, Dembélé et al. (2020) and Dembélé and Zwart (2016) showed that ARCv2 is among the most suitable database in picturing precipitation over the Volta basin and also over Burkina Faso. The quality of ARC.2 data after correction by Empirical Quantile Mapping (EQM) was not significantly improved. Finally, ARC.2 was directly used to fill the gaps in the rainfall data for the rain gauges. The Thiessen polygon method was used to spatialize the rainfall over the watershed. The Thiessen polygon method was selected because it is suitable for our study area (Olawoyin and Acheampong, 2017) given the insufficient number of rain gauges and their heterogeneous distribution over the watershed.

The comparative analysis of spatial PE databases (CRU TS v 4.03 and TerraClimate) with PE data from the two synoptic stations (provided by ANAM) through the Mann-Whitney test (at the 5% level) showed that:

- there is no significant difference between annual PE provided by ANAM and those from TerraClimate (p-value = 0.0890);
- annual PE of CRU TS v 4.03 are significantly different from those provided by ANAM (p-value $<$ 0.0001).

TerraClimate database also provides AE data at the same resolution and for the same period as PE. Therefore, the TerraClimate database was considered as the source for PE and AE in this study.

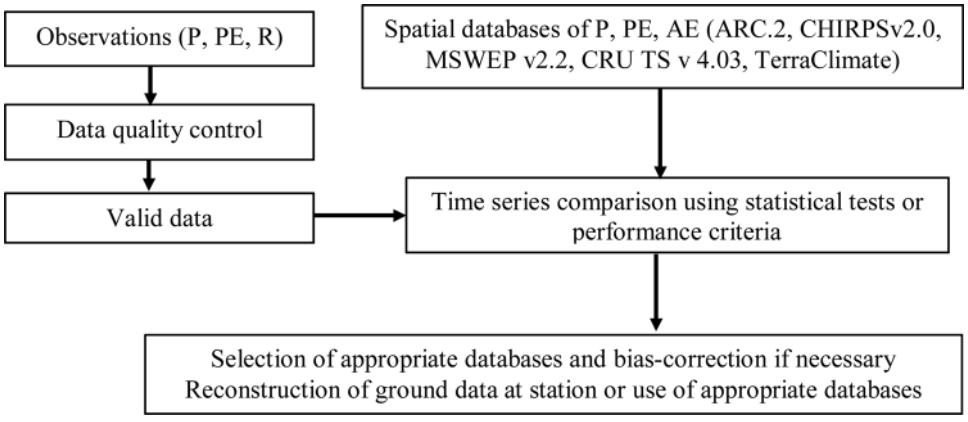

Fig. 2. Flowchart of hydro-climatic data processing in this study: P (precipitation), PE (potential evapotranspiration), R (surface runoff) and AE (actual evapotranspiration).

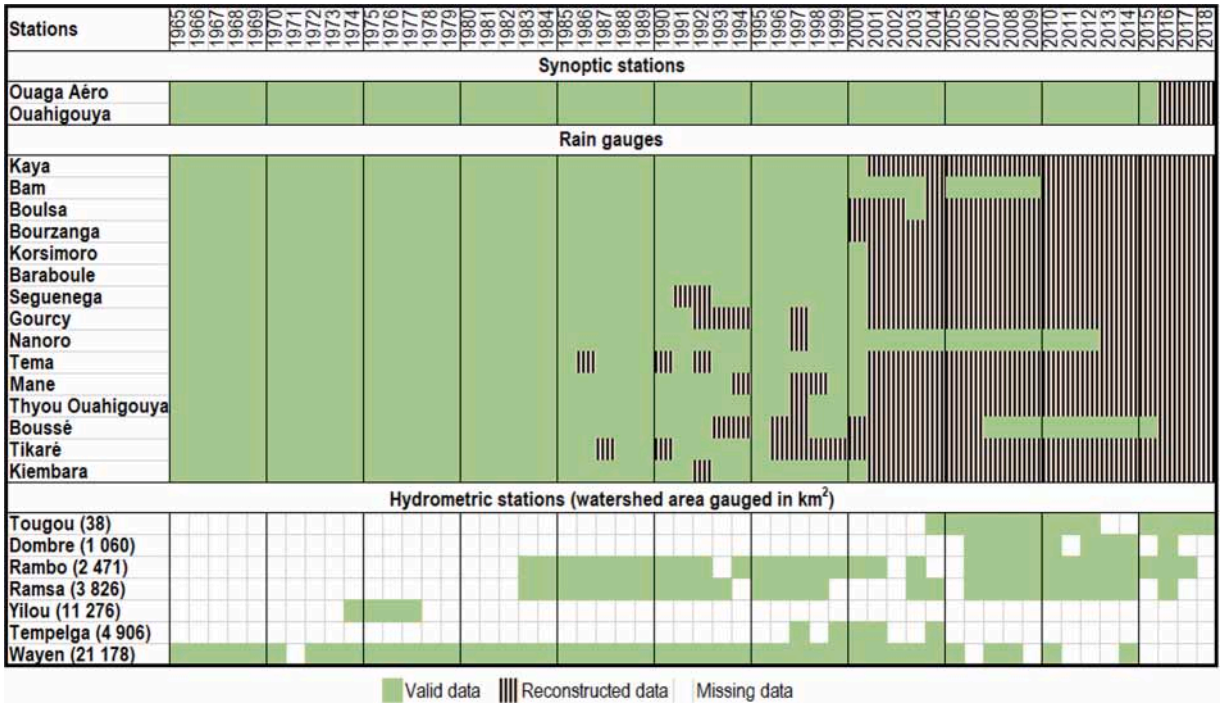

Fig. 3. Hydro-meteorological data of ground stations.

Table 1
Overview of datasets used in this study.

Datasets	Type of data	Spatial resolution	Temporal resolution	Period	Source
Meteorological observations	P, PE	Point data (17 stations)	Daily	1965–2015	Boyer et al. (2006); ANAM
Surface runoff observations	R	Point data (7 stations)	Daily	1965–2017	DGRE, 2iE
Dams	Characteristics	371 dams	NA	NA	
Filling of dams	Monitoring (volume stored)	2 dams (Ziga and Dourou)	Daily	1996–2018	DGRE
Water withdrawals	Withdrawals volume	Point data (Ziga)	Monthly	2004–2018	ONEA
ARC v2	P	10 km × 10 km	Daily	1983–2018	Novella and Thiaw (2012)
CHIRPS v2.0	P	5 km × 5 km	Daily	1981–2018	Funk et al. (2014)
MSWEP v2.2	P	10 km × 10 km	Daily	1979–2017	Beck et al. (2019)
TerraClimate	P, PE, AE	1/24° (~4 km)	Monthly	1958–2018	Abatzoglou et al. (2018)
CRU TS v 4.03	PE	0.5°×0.5°	Monthly	1901–2017	University Of East Anglia Climatic Research Unit (CRU) et al. (2020)
Demography	demography	Municipality scale	1985, 1996 and 2006	NA	INSD
NDVI data	NDVI	8 km × 8 km	2-weekly	1981–2015	National Center for Atmospheric Research Staff (2018); Pinzon and Tucker (2014)
DEM data	Digital Elevation Data	30 m	NA	NA	(ALOS, 2020)

Note: ANAM : Agence Nationale de la Météorologie ; DGRE: Direction Générale des Ressources en Eau; 2iE: Institut International d'Ingénierie de l'Eau et de l'Environnement; ONEA : Office National de l'Eau et de l'Assainissement ; INSD : Institut National de la Statistique et de la Démographie.

2.3. Altitude, vegetation and demographic data

The Digital Elevation Model (DEM) ALOS World 3D (AW3D), from the Japan Aerospace Exploration Agency (JAXA), was used in this study. From this DEM data, the boundaries of the nested watersheds were extracted. The demographic data from 1985, 1996 and 2006 national censuses of the population were provided by INSD (Table 1). The population density was evaluated for administrative and territorial units found within the Nakanbé watershed. The Normalized Difference Vegetation Index (NDVI) data used in this study is from Pinzon and Tucker (2014) and is based on NOAA (National Oceanic and Atmospheric Administration) and EUMETSAT (European Organization for the Exploitation of Meteorological Satellites) records, provided at 8 km × 8 km resolution over the period

1981–2015.

3. Methodology

Fig. 4 outlines the methodological framework used in this study. Firstly, Pettitt test and segmentation procedure were applied to split the study period into pre-change (baseline period) and change (impact periods). Sensitivity analysis based on the partial derivative allowed selecting the most suitable Budyko-type model for West African Sahel (WAS). Secondly, the suitable Budyko-type model chosen was used to quantify the impacts of CC/EC on the water resource of the seven nested watersheds through elasticity and decomposition methods. A specific elasticity method developed allowed quantifying the individual impacts of CC and EC and the impact of their interaction. Finally, correlation and regression research techniques were applied to explore the spatial variability of the impacts and the relationship between the parameter of Budyko and the vegetation coverage (*M*).

3.1. Breakpoint detection methods

The Pettitt test (Pettitt, 1979) and the segmentation procedure (Hubert et al., 1989) for the detection of one or more breakpoints respectively were applied to annual hydro-climatic and environmental time series data. Herein, the results obtained from the segmentation procedure were considered only in the occurrence of numerous breaks and the results of the Pettitt test were considered for single-breaks. We limited the use of the segmentation procedure due to the ambiguity around the significance level of its results (Hubert et al., 1989): there is not a precise p_value assigned to each result.

3.2. Quantification of impacts of climate and environmental changes on water resources based on Budyko framework

Assuming negligible in the long term, changes in subsurface water storage and net heat transfer between the land surface and the vadose zone (root zone), water and energy balances at the watershed scale become Eq.(1) (Sposito, 2017).

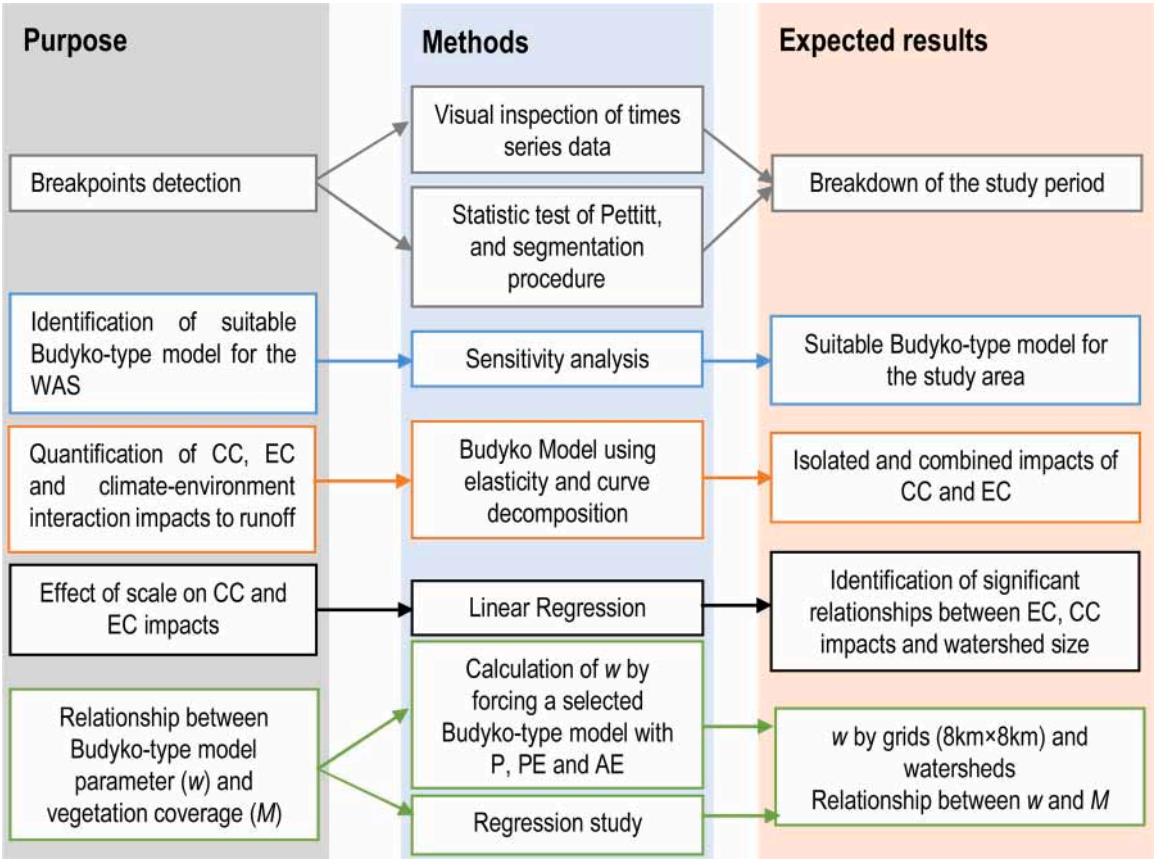

Fig. 4. Methodological framework used in this study; WAS: West Africa Sahel, CC: climate change, EC: environmental change, P: precipitation, PE: potential evapotranspiration, AE: actual evapotranspiration.

$$\begin{cases} AE = P - R \\ AE = PE - \dfrac{h}{L} \Longrightarrow AE = f(P, PE) \end{cases} \quad (1)$$

where P[L/T] = Precipitation, AE[L/T] = Actual evapotranspiration, R[L/T] = Runoff, PE[L/T] = Potential evapotranspiration, h[M/T^3] = Sensible heat flux and L[M·L^{-1}·T^{-2}] = Latent heat of vaporization.

Dividing the terms in Eq.(1) by the precipitation (P) gives Eq.(2), which expresses the conceptual framework of Budyko (Budyko, 1974).

$$\begin{cases} \dfrac{AE}{P} = f\left(\dfrac{PE}{P}\right) \\ \dfrac{AE}{P} = f(\varphi) \end{cases} \quad (2)$$

where φ (ratio between PE and P) is the aridity index. The aridity index indicates the climate type and is the most widely used similarity measure (Blöschl et al., 2013). Wetlands are characterized by low aridity index ($\varphi < 0.76$) while an aridity index greater than 1.35 indicates an arid zone (MCVicar et al., 2012).

This framework is the basis of several models for estimating actual evapotranspiration (Dey and Mishra, 2017). Budyko parametric models (Table 2) have been widely used to quantify the impacts of CC and human interferences on the hydrological response of watersheds (Dey and Mishra, 2017; Li et al., 2019; Liu et al., 2019; Teuling et al., 2019; Zhang et al., 2019a).

The Budyko-type parametric models (Table 2) show that, in a given watershed, the evaporative index ($\frac{AE}{P}$) is a function of the aridity index (φ) and the parameter (e). Therefore, Eq.(2) can be rewritten as in Eq.(3).

$$\frac{AE}{P} = f(\varphi, e) \quad (3)$$

where φ is the aridity index and e is the Budyko-type model parameter

The methods for assessing impacts used in the Budyko approach are climate elasticity and Budyko curve decomposition.

3.2.1. *Budyko curve decomposition for quantifying impacts of climate change and human interferences on water resources*

In the Budyko framework, based on global data, it has been shown that, under natural conditions (without human interference), the evolution of the state of a watershed follows the Budyko curve (Budyko, 1974). Climate change (CC) leads to changes in aridity and evaporative indexes (A to B' in Fig. 5) of the watersheds (Wang and Hejazi, 2011), which translates as horizontal and vertical shifts, while human interferences cause only vertical shifts. These shifts could be explained by the fact that the aridity index ($\varphi = PE/P$) and the evaporative index (AE/P) depend on the climate, whereas human activities only affect AE (Tomer and Schilling, 2009). Based on

Table 2
Parametric models based on the Budyko framework (Dey and Mishra, 2017; Du et al., 2016; Greve et al., 2016).

Authors	f	Advantages	Limitations
Fu (1981)	$1 + \varphi - (1+\varphi^{w})^{1/w}$	Based on dimensional analysis with rigorous mathematical reasoning and is the most used	Cannot be used when $\frac{AE}{P} \geq 1$
Choudhury (1999)	$(1+\varphi^{-n})^{-1/n}$	Generalized form of Pike (1964) equation	Cannot be used when $\frac{AE}{P} \geq 1$ and not used a lot
Zhang et al. (2001)	$\frac{1+m\varphi}{1+m\varphi+\varphi^{-1}}$		Cannot be used when $\frac{AE}{P} \geq 1$ and not used a lot
Porporato et al. (2004)	$1 - \frac{\frac{\gamma-\varphi}{\varphi\gamma}\ \varphi\ e^{-\gamma}}{\Gamma\left(\frac{\gamma}{\varphi}\right) - \Gamma(\frac{\gamma}{\varphi}, \gamma)}$	Stochastic model	Useful when the saturation runoff formation mechanism is dominant
Wang and Tang (2014)	$\frac{1+\varphi-\sqrt{(1+\varphi)^2 - 4\psi(2-\psi)\varphi}}{2\psi(2-\psi)}$	Based on a generalization of the proportionality hypothesis of the SCS model	Cannot be used when $\frac{AE}{P} \geq 1$ and not used a lot
Du et al. (2016)	$1 + \varphi - (1+\varphi^{u}+\lambda)^{1/u}$	Extension of Budyko hypothesis under unsteady state ($\frac{AE}{P} \geq 1$)	λ is not analytically estimable and if $\frac{AE}{P} < 1$, it joins Fu (1986)
Greve et al. (2016)	$1 + \varphi - (1+(1-y_0)^{k-1}\varphi^{k})^{\frac{1}{k}}$	Extension of Budyko hypothesis under unsteady state ($\frac{AE}{P} \geq 1$)	if $\frac{AE}{P} < 1$, it joins Fu (1986)

Note: In the model of Porporato et al. (2004), $\Gamma()$ is the gamma function and $\Gamma(.,.)$ is the complete gamma function.
w, n, m, γ, ψ, u, k, λ and y_0 are dimensionless fitting parameters. w, n, m, γ, ψ, u and k consider environmental change while λ and y_0 are related to the new boundary condition when evaporative index excess 1. w and n reflect the watershed characteristics (vegetation type, soil properties and topography). m is the plant-available water coefficient. γ takes into account the effect of the precipitation average height and the soil water holding capacity. The parameter ψ is the ratio of two dimensionless numbers, i.e., the ratio of the initial evaporation ratio to the Horton index. u and k are similar to the parameter w of Fu model.

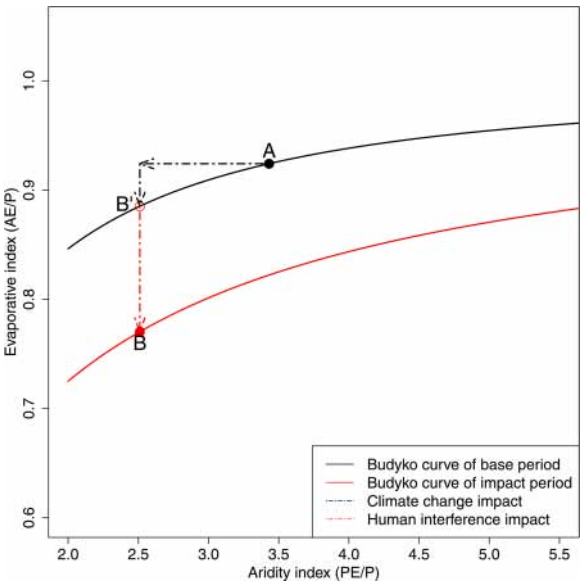

Fig. 5. Quantification of impacts based on the Budyko curve decomposition method. A(PE_1/P_1,AE_1/P_1), B'(PE_2/P_2,AE_2'/P_2), B(PE_2/P_2,AE_2/P_2). PE = Potential evapotranspiration, P = Precipitation and AE = Actual evapotranspiration.

the above assumptions, Wang and Hejazi (2011) have shown that the contributions of CC (C_{Cde}) and human interferences (H) on the runoff change in a watershed (which has gone from state A to state B, Fig. 6) can be quantified by Eq.(4).

$$\begin{cases} H = \dfrac{\Delta R_H}{\Delta R} = \dfrac{P_2}{\Delta R}\left(\dfrac{AE'_2}{P_2} - \dfrac{AE_2}{P_2}\right) \\ C_{Cde} = \dfrac{\Delta R_C}{\Delta R} = \dfrac{P_2}{\Delta R}\left(1 - \dfrac{AE'_2}{P_2}\right) - \dfrac{R_1}{\Delta R} \end{cases} \tag{4}$$

where R_1, ΔR, ΔR_C *and* ΔR_H are respectively average annual values of runoff over baseline period, total runoff change, runoff change due to CC and due to human interferences.

The following procedures were adopted to evaluate the isolated contributions of CC (C_{de}) and human interferences (H) to runoff change in the nested watersheds of the Nakanbé River. The average annual aridity and evaporative indexes for baseline and impact periods were, first, calculated based on the yearly average of *P, PE and AE*. Secondly, the selected Budyko-type model was forced with the average of the aridity and evaporative indexes values over the baseline period to estimate the model parameter (e). Thirdly, the estimated parameter (e) over the baseline period was used to compute the evaporative index due to climate change only (AE'_2 in Fig. 5). Finally, the contribution of each factor (climate and human interference) to runoff change was quantified, as shown in Eq.(4).

3.2.2. Elasticity-based method to quantify impacts of climate change, environmental change and climate-environment interaction on water resources

By deriving the runoff expression (from Eq (1) and (3)), the elasticity coefficients of climate (β) and environment (ε_e), as well as the contributions of CC (C_C), EC (C_E) and interaction of climate-environment (C_{ICE}) were obtained (Eq.(5)). The details of the derivation procedure are provided in the Appendix.

$$\begin{cases} \Delta R = \left[(1+\beta)\dfrac{\Delta P}{P_1} - \beta\dfrac{\Delta PE}{PE_1}\right]R_1 + \varepsilon_e\dfrac{\Delta e}{e}R_1; \beta = \dfrac{\varphi}{1-f(\varphi,e)}\dfrac{\partial f}{\partial \varphi} and \varepsilon_e = \dfrac{-e}{1-f(\varphi,e)}\dfrac{\partial f}{\partial e} \\ C_C = \left[(1+\beta)\dfrac{\Delta P}{P_1} - \beta\dfrac{\Delta PE}{PE_1}\right]\dfrac{R_1}{\Delta R} \\ C_E = \varepsilon_e\dfrac{\Delta e}{e_1}\dfrac{R_1}{\Delta R} \\ C_{ICE} = 1 - C_C - C_E \end{cases} \tag{5}$$

where C_C, C_E and C_{ICE} are respectively the contributions of CC, EC and interaction of climate-environment to runoff change (ΔR). e_1, R_1, P_1 *and* PE_1 are respectively average values of the parameter, runoff, precipitation and potential evapotranspiration over the baseline period. Δe, ΔP *and* ΔPE are respectively, the variations in the parameter, precipitation and potential evapotranspiration between baseline and impact periods.

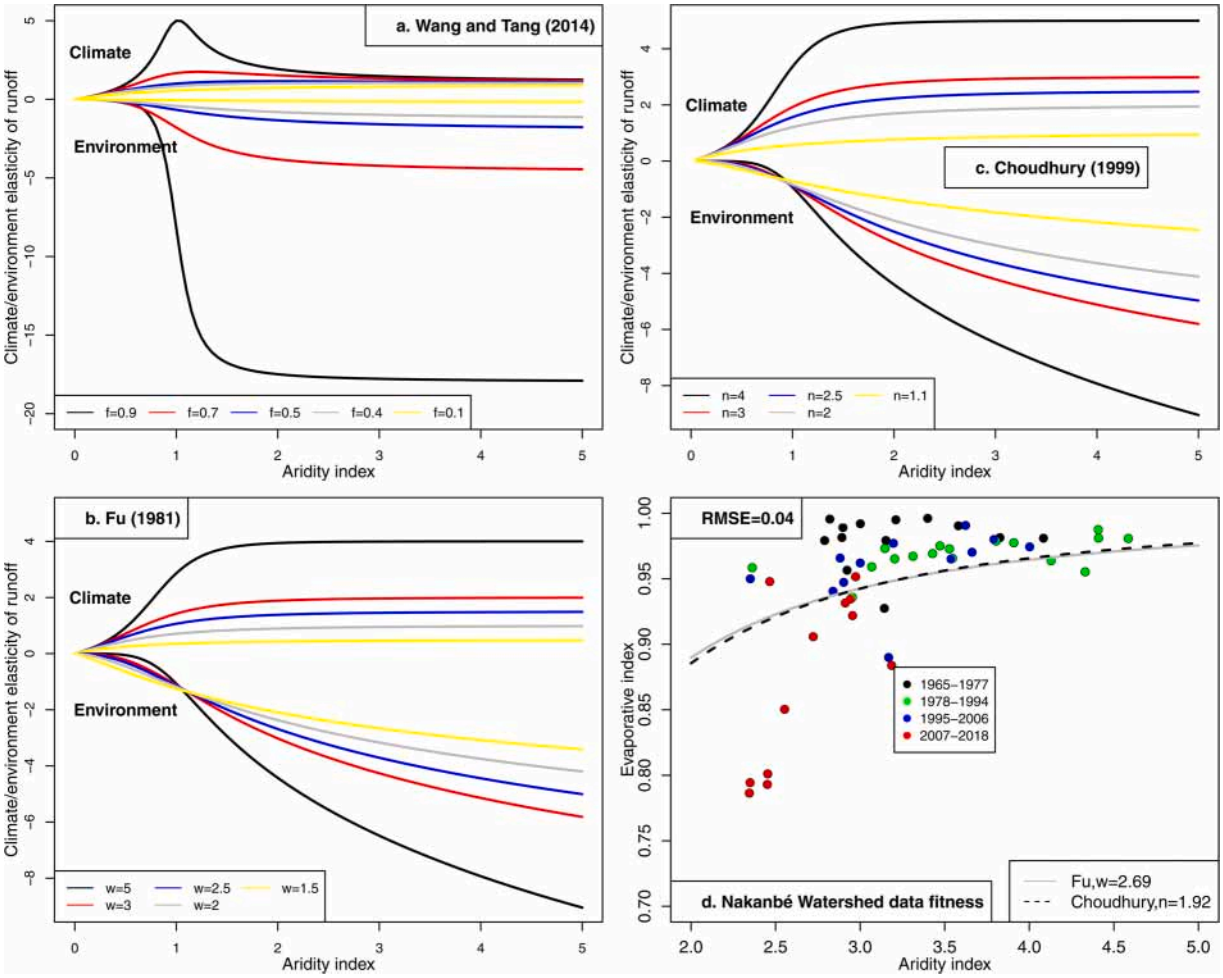

Fig. 6. Sensitivity analysis of models ((a) - Wang and Tang (2014), (b) - Fu (1981), (c) - Choudhury (1999)) and Nakanbé Watershed data fitness to Fu and Choudhury models (d).

The derivation of the Budyko function does not consider the interactions between the variables P, PE and e. Therefore, the resulting elasticity coefficients are assumed to be the eigenvalues of the climate and environment elasticities. These coefficients were used to quantify the isolated impact of CC (C_C) and EC (C_E) on surface runoff variation. As such, the difference between the total change in surface runoff and the isolated contributions of climate and environmental change can be attributed to the climate-environment interaction ($C_{ICE} = 1\text{-}C_C\text{-}C_E$). Indeed, it is already acknowledged that climate and environment are interrelated with each other (Dearing, 2006; Gao et al., 2014). However, it should be admitted that the contribution of the climate-environment interaction (C_{ICE}) deduced here, might include model uncertainty. Further work is needed to estimate this uncertainty when the data requirement is met.

The elasticity coefficient of runoff to climate (β) is similar to that obtained by Arora (2002). The elasticity coefficients β and ε_e, which denote the level of sensitivity of runoff to climate (*P* and *PE*) and environmental changes (respectively), were used to analyze the sensitivity of the Budyko-type models (Table 1) to the aridity index in order to identify the most suitable ones for the study area.

3.3. *Identification of Budyko models adapted to the Sahelian context*

The identification of Budyko models adapted to the Sahelian context was based on sensitivity analysis of Budyko type models to aridity index, as the West African Sahel is characterized by a high aridity index. It should be recalled that the elasticity coefficients (β and ε_e) are also sensitivity coefficients (McCuen, 1974) because they are based on the derivative of each Budyko function.

Among all the models based on the framework of Budyko, Fu (1981) model has been the most widely used (Fathi et al., 2019). Furthermore, a comparative study (Zhang et al., 2004) has shown that the Fu model is better than that of Zhang et al. (2001). The equation of Porporato et al. (2004) is useful when the saturation runoff formation mechanism is dominant over the Hortonian runoff (Table 2). As the hydrological response of watersheds in WAS is characterized by the Hortonian runoff generation (Casenave and Valentin, 1991), the models, which can be used, are those of Choudhury (1999); Fu (1981) and, Wang and Tang (2014). The two-parameter models (Du et al., 2016; Greve et al., 2016) are an extension of the model of Fu (1981). A sensitivity analysis, based on

elasticity coefficients of runoff to aridity index, was carried out to identify the most suitable models for the study area among those of Fu, Choudhury and Wang and Tang.

Fig. 6 (a, b and c) shows the evolution of the elasticities of climate (β) and environment (ε_e) as a function of aridity index (φ) for each of the three models. Choudhury (1999) and Fu (1981) models showed similar results: β reaches its highest values from $\varphi = 2$, while ε_e increases continuously with φ. With Wang and Tang (2014) model, β and ε_e are more sensitive when $\varphi < 2$. Therefore, this model does not appear relevant for our case study and even for the WAS in general, where the aridity index is likely to reach higher values ($\varphi > 2$, as shown in Fig. 6.d). The models of Fu and Choudhury models seem to be the most suitable based on sensitivity analysis.

The fitness quality of the Nakanbé watershed at Wayen data to Fu and Choudhury models over the period 1965–2018 was assessed using the Root Mean Square Error function (Eq. (6)).

$$RMSE = \sqrt{\frac{1}{N}\sum_{i=1965}^{2018}\left[\left(\frac{AE}{P}\right)_i - \left(\widehat{\frac{AE}{P}}\right)_i\right]^2} \tag{6}$$

where N is the data series length; $\left(\frac{AE}{P}\right)_i - \left(\widehat{\frac{AE}{P}}\right)_i$ represents the difference between simulated and observed evaporative indexes. (6)

The result showed that both models (Fu and Choudhury) fit well to the data (Fig. 6.d) with the same Root Mean Square Error (RMSE = 0.04). The lag in the data over the period 2007−2018 is certainly due to the effect of environmental change because Budyko functions adjustment by a fixed parameter implies neglecting the watershed environmental change. The Fu model was applied in this study because it is mathematically based and the most widely used (Table 2)

3.4. Exploring the relationship between Fu model parameter (w) and vegetation coverage (M)

The vegetation coverage (M) is one of the main characteristics of the land surface, which largely controls the spatial variability of the parameter relating to the environmental conditions in Budyko-type models (Ning et al., 2019; Teuling et al., 2019; Zhang et al., 2004, 2001, 1999). In this study, remotely sensed vegetation information was used to estimate the vegetation coverage (Li et al., 2013) through the Normalized Difference Vegetation Index ($NDVI$) as shown in Eq.(7):

$$M = \frac{NDVI - NDVI_{min}}{NDVI_{max} - NDVI_{min}} \tag{7}$$

where M indicates the vegetation coverage; $NDVI_{max}$ and $NDVI_{min}$ are NDVI values for dense forest (0.80) and bare soil (0.05),

Table 3
Breakpoints in annual hydro-climatic time series data in the nested watersheds of Nakanbé at Wayen over the period 1965-2018.

Nakanbé River Watersheds	Variables (mm)	Pettitt test				Segmentation procedure		
		p-value	Breakpoints and mean before / after (Significance level: 10 %)			Breakpoints and mean before/ after		
			Year	Before	After	Year	Before	After
Wayen (21,178 km^2)	P	0.000	1997	602.0	740.6	1997	602.0	710.1
						2014	710.1	869.8
	PE	0.018	1982	2,015.4	2,081.0			
	R	0.067	1977	9.9	20.1/ 23.5*			
Yilou (11,276 km^2)	P	0.000	2000	596.2	770.4	2000	596.2	734.6
						2014	734.6	895.7
	PE	0.034	1982	2,019.2	2,079.3			
Tempelga (4,906 km^2)	P	0.009	1997	586.4	692.5			
	PE	0.024	1982	2,042.8	2,109.5			
Ramsa (3,826 km^2)	P	0.000	1993	543.1	709.6	1981	587.6	451.5
						1990	451.5	620.5
						2006	620.5	792.5
	PE	0.072	1982	2,057.7	2,115.0			
	R	0.106						
Rambo (2,471 km^2)	P	0.000	1997	533.4	707.5	1969	650.2	497.2
						1993	497.2	657.0
						2014	657.0	870.0
	PE	0.082	1982	2,067.8	2,126.0			
	R	0.110						
Dombré (1,060 km^2)	P	0.004	1990	571.4	736.1			
	PE	0.063	1982	2,036.8	2,091.5			
Tougou (38 km^2)	P	0.004	1990	571.1	736.5			
	PE	0.070	1982	2,050.1	2,105.2			

Empty tiles indicate non-detection of breakpoint.
* Considering the runoff reconstituted after the construction of Ziga and Dourou dams.

respectively.

The relationship between w and M was assessed through regression. For this purpose, the values of the parameter *w* were calculated by forcing the Budyko-type model of Fu (1981) with long-term average data of P, PE and AE at watersheds (7) and grid (276 NDVI grids) scale.

The regressions performance was assessed through the coefficient of determination R^2 (Eq.(8)).

$$R^2 = \left[\frac{\sum_{i=1}^{283} (M_i - \overline{M})(w_i - \overline{w})}{\sqrt{\sum_{i=1}^{283} (M_i - \overline{M})^2} \sqrt{\sum_{i=1}^{283} (w_i - \overline{w})^2}} \right]^2 \quad (8)$$

where $\overline{M}$ and $\overline{w}$ are the averages (over the 276 grids and 7 watersheds, i.e. 283) of vegetation coverage (M) and the Fu model parameter (w), respectively. (8)

4. Results

4.1. Hydro-meteorological and environmental changes in the Nakanbé watershed at Wayen

Table 3 presents the results of breakpoints detection tests performed on the annual hydro-meteorological time series in seven nested watersheds of the Nakanbé River. We investigated the change in runoff through the three gauges with at least 20 valid years of records (Wayen, Ramsa and Rambo). The Pettitt test identified 1977 and 1982 as break-years in the time series data of R and PE respectively, whereas various breakpoints during 1990–2000 were identified in P time series in the nested watersheds of the Nakanbé River. Additionally, the segmentation procedure identified 1969, 1981, 2006 and 2014 as breakpoints in precipitation time series. As the period 2015–2018 is relatively short, 2014 was not considered as a breakpoint year. The breakpoints years 1969 and 1981 showed a significant reduction in precipitation, while the breakpoints over the period 1990–2000 and in 2006 indicated a significant increase.

As shown in Fig. 7.a for the whole watershed, annual precipitation decreased from 1965 to 1981, reaching its lowest values during the 1981–1990 period. Since 1990, a recovery in precipitation has been observed, which intensified from 2007. The runoff coefficient of the Nakanbé watershed at Wayen increased from 1965 to 2018 (Fig. 8.b) despite the drought of the 1980s and the impoundment of Dourou (100 million m^3 in 1995) and Ziga (200 million m^3 in 2000) dams. In the absence of these two dams, the average runoff coefficient over the period 2007–2014 would be 6 % against 1.5 % over the period 1965–1977. The increase in runoff despite the decrease in precipitation over the period 1965–1990 is reminiscent of the first Sahelian hydrological paradox (Descroix et al., 2018; Wendling et al., 2019).

The environmental change and its spatial variability were assessed through the vegetation coverage (M) and NDVI. Significant spatial variability was observed in the vegetation cover of the Nakanbé watershed at Wayen (Fig. 8.a). The trend in NDVI from 1982 to 2015 (Fig. 8.b) showed a decrease from 1982 to 1984, an increase until 1993 and relative stability since 1993. The test of Pettitt

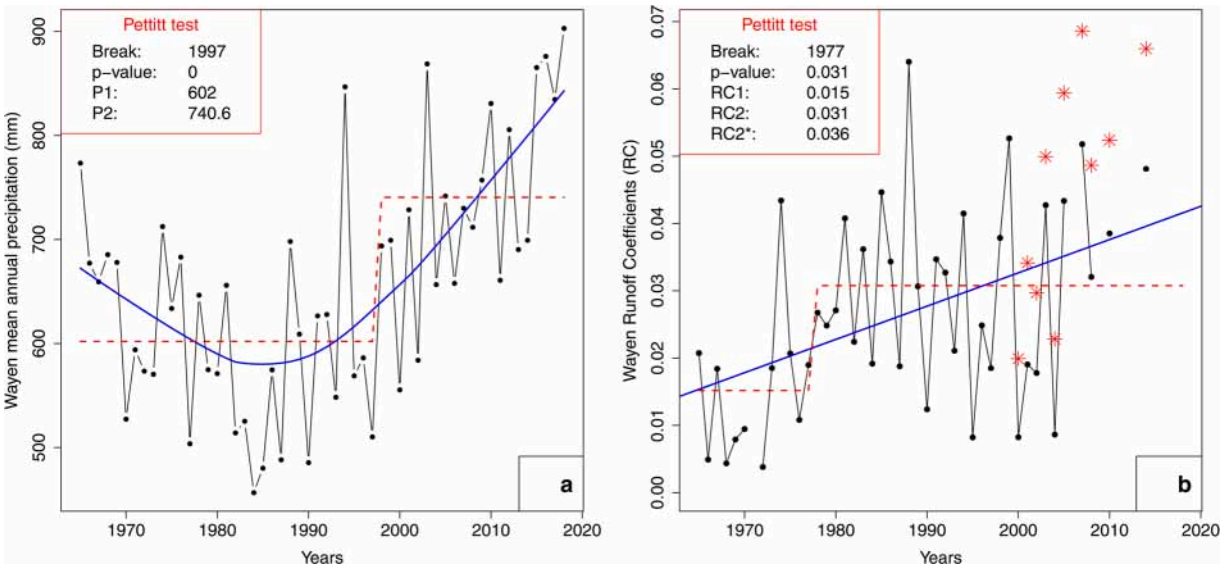

Fig. 7. Evolution of annual precipitation (a) and runoff coefficient (b) in Nakanbé watershed at Wayen. Blue curve/line shows the trend and red dashed lines, the breakpoints. Red stars represent the reconstituted runoff coefficient (RC2*) after the impoundment of Ziga and Dourou dams, P1/RC1 refers to the period before breakpoint and P2/RC2 refers to the period after breakpoint. P designated precipitation and RC runoff coefficient.

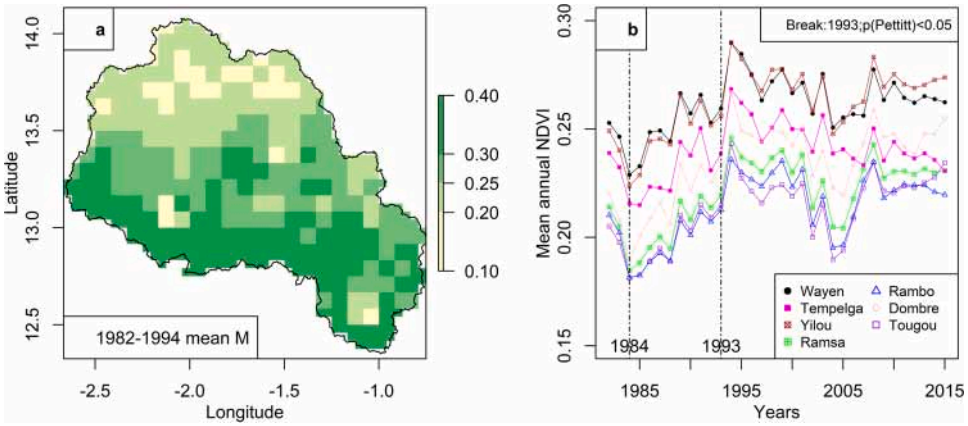

Fig. 8. Vegetation spatio-temporal variability in Nakanbé watershed at Wayen area: (a) - vegetation coverage (M), (b) - NDVI trends.

indicated 1993 as a breakpoint year in the average NDVI time series for all sub-watersheds (p-value < 0.05). The increase in runoff coefficient over the period 1994–2018 (Fig. 7.b) despite the re-greening (Fig. 8.b) is reminiscent of the second Sahelian hydrological paradox (Descroix et al., 2018)

It was also shown that population growth led to decreased vegetation in these locations (Diello, 2007). Table 4 indicates that from 1985 to 2006, the population density increased in all watersheds. The average population density of the watershed ranged from 50 inhabitants per square kilometer (hbts/km^2) in 1985 to 62 in 1996 and 79 in 2006, with an important spatial variability. The sub-watershed gauged by Dombré station exhibits the highest densities (98/122/156 hbts/km^2 respectively in 1985/1996/2006) while the Rambo sub-watershed has the lowest densities (32/45/56 hbts/km^2 respectively in 1985/1996/2006). It is instructive to point out that the Dombré sub-watershed shelters Ouahigouya city, the fifth-largest city in Burkina Faso.

In summary, the evolution of hydro-meteorological and environmental time series showed significant breaks before 1982 (in PE, P and R), over the period 1990–2000 (P, NDVI with the impoundment of the two large dams) and after 2006 (P). Based on these breakpoints, the study period was divided into one baseline period (1965–1977) and three impacted periods (1978−1994, 1995−2006 and 2007−2018). In the Nakanbé watershed at Wayen, the period 1978−1994 was the driest and characterized by the highest aridity indexes (Fig. 9) and lowest NDVI values (Fig. 8.b). The periods 1995−2006 and 2007−2018 compared to 1978−1994 were characterized by a decrease in the aridity index (Fig. 9.b to d). Overall, from 1965 to 2018, runoff has increased in all nested watersheds. However, over the period 1978−1994, runoff derived from the water balance exhibited a decrease compared to the period 1965–1977 in the sub-watersheds of Rambo (28.59 mm vs. 41.82 mm) and Ramsa (38.26 mm vs. 43.29 mm).

4.2. Separated and combined effects of climate and environmental changes on water resources in the nested watersheds of Nakanbé

Based on the identified sub-periods (subsection 4.1), the elasticity and decomposition methods (Eq.(4) and (5)) were applied to quantify the contributions of each factor (climate and environmental changes) to runoff change. The decomposition method made it possible to quantify the impacts of climate change (C_{Cde}) and human interferences (H) and the elasticity method developed in this study allowed the quantification of the impacts of CC (C_C), EC (C_E) and climate-environment interaction (C_{ICE}). The analysis of the results showed that H includes C_E and C_{ICE}. Fig. 10 showed that elasticity and decomposition-based methods gave similar results ($R^2 = 0.99$).

In the following, only the results based on the elasticity method are presented (Table 5). The elasticity coefficients analysis showed that runoff is more than twice as sensitive to environmental change (EC) than climate change (CC). The negative value of impact indicates a contribution in the opposite direction to the runoff variation. The analysis of the individual and combined contributions of CC and EC to runoff changes showed that:

Table 4
Demography in nested watersheds of Nakanbé River.

Nakanbé River nested Watersheds	Population density (inhabitants/km^2)		
	1985	1996	2006
Wayen (21,178 km^2)	49.82	61.97	79.01
Yilou (11,276 km^2)	54.16	66.62	84.89
Tempelga (4,906 km^2)	40.86	49.64	66.27
Ramsa (3,826 km^2)	50.65	66.72	84.17
Rambo (2,471 km^2)	31.81	44.88	55.75
Dombré (1,060 km^2)	97.60	121.83	156.04
Tougou (38 km^2)	56.97	62.94	79.30

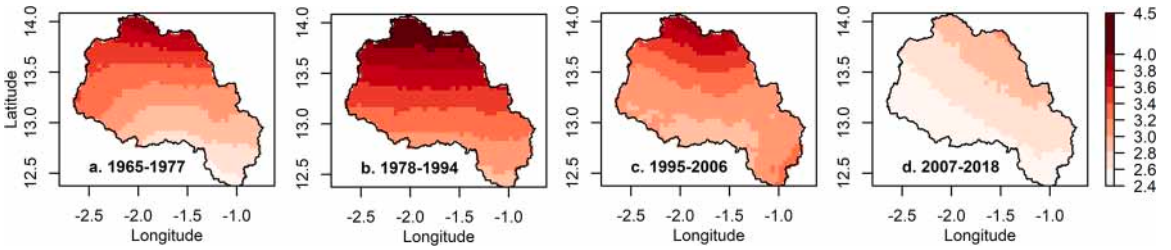

Fig. 9. Spatio-temporal variability of aridity index in Nakanbé watershed at Wayen over the baseline (a) and impacted periods (b, c, d).

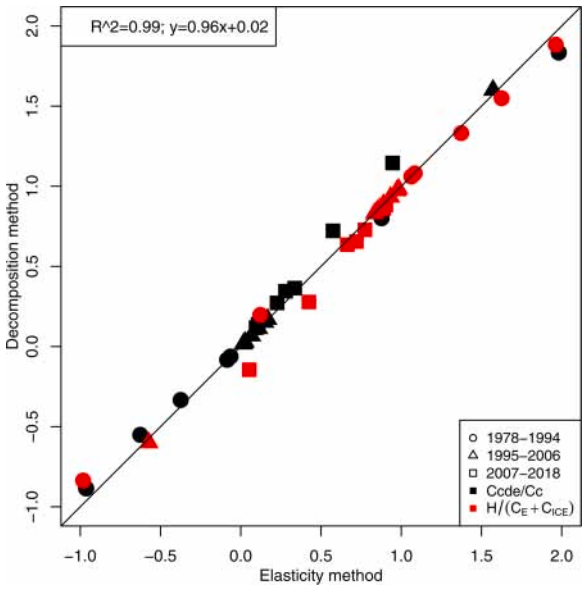

Fig. 10. Cross comparison of results from decomposition and elasticity methods. Ccde and Cc are the impacts of climate change quantified respectively by decomposition and elasticity methods. H is the impact of human interferences (decomposition method) and C_E+C_{ICE} is the sum of the impacts of environmental change and climate-environment interactions (elasticity method).

Table 5
Elasticity coefficients and contributions of climate and environmental change to runoff change relative to the baseline period (1965-1977).

Nested watersheds	Elasticity coefficients		Contributions (%)								
			1978−1994			1995−2006			2007−2018		
	β	ε_e	C_C	C_E	C_{ICE}	C_C	C_E	C_{ICE}	C_C	C_E	C_{ICE}
Wayen	2.33	−4.85	−63	133	29	2	63	36	10	23	68
Yilou	2.09	−4.64	−37	102	35	3	41	56	11	21	68
Ramsa	1.33	−3.96	198	−93	−5	157	−56	−1	95	−9	15
Tempelga	1.55	−4.05	−96	175	21	7	82	11	34	40	26
Dombré	1.43	−3.99	−8	75	33	15	58	27	58	14	28
Rambo	1.31	−4.01	88	26	−14	17	60	23	23	27	50
Tougou	1.34	−3.90	−6	71	35	11	57	32	28	25	47

β=Runoff elasticity coefficient to climate; ε_e= Runoff elasticity coefficient to the environment; C_C, C_E and C_{ICE} designate the respective contributions of climate change (CC), environmental change (EC) and climate-environment interaction to runoff change. Partial contributions greater than 100 % are due to negative partial contributions and $C_C+C_{ICE}+C_E = 100$ %.

- Over the period 1978−1994, EC was the leading cause of the increased runoff at Wayen, Yilou, Tempelga, Dombré and Tougou. In the Ramsa and Rambo watersheds, the drought (increased aridity) was dominant and decreased the surface runoff.
- From 1995 to 2018, the precipitation recovery contributed positively to the increase in runoff in all watersheds ($C_C > 0$ and $\Delta R > 0$).
- During the period 1995−2006, the contribution of EC was the highest in all watersheds except Ramsa and Yilou. In the Ramsa watershed, CC was the predominant factor, while the climate-environment interaction was the most important in the Yilou watershed.

- Over the period 2007−2018, climate-environment interaction has been the main factor causing the increase in surface runoff in four watersheds (Wayen, Yilou, Rambo and Tougou) against two for CC (Ramsa and Dombré) and one for EC (Tempelga).
- Between 1978 and 2018, the impact of climate-environment interaction increased.

The seven nested Nakanbé watersheds at Wayen (with surface ranging from 38 to 21,178 km^2) were considered to assess the spatial scale effect. Fig. 11 shows that the absolute value of the elasticity coefficient is proportional to the size of the watersheds. However, the low regression coefficients ($5{\cdot}10^{-5}$ for climate and $-4{\cdot}10^{-5}$ for the environment) explain the non-detection of a significant relationship between the impacts and the size of the watersheds.

4.3. *Evolution of the state of Nakanbé nested watersheds under the Budyko framework from 1965 to 2018*

Fig. 12 shows the evolution of the states of the seven Nakanbé nested watersheds under the Budyko framework and helps in understanding the effects of CC and EC on water resources (Table 5). According to Wang and Hejazi (2011), Fig. 12.a shows the impacts of possible watershed state shifts in the Budyko framework. A decrease or increase in aridity index implies the respectively positive or negative contribution of CC to runoff increase. Over the period 1978–1994, the increase in aridity index (all the watersheds shifted to the right in Fig. 12.b to h) justifies the negative contribution of CC to the increase in runoff. The precipitation recovery (all watersheds moved to the left in Fig. 12.b to h) caused the positive contribution of CC to the increase in runoff since 1995. Also, Fig. 12. (b to h) shows that the nested watersheds located in the northwest (Ramsa, Rambo, Dombré and Tougou) have the lowest parameter w. The northern part of the watershed is globally characterized by a very low vegetation cover (Fig. 8.a) and high aridity indexes (Fig. 9). Therefore, it could be concluded that low vegetation cover coupled with a high aridity index lead to low *w* values. In the Budyko framework, unilateral decrease/increase in evaporative index translates into a decrease/increase in the model parameter (*w*), leading to positive/negative contribution of human interferences to runoff change, respectively. The decrease in vegetation can be caused by direct anthropogenic actions (deforestation) or by CC. Thus, a change in *w* can be attributed to direct anthropogenic activities or climate-environment interactions. Therefore, the parameter w is a potential global environmental indicator, including direct and indirect changes in the environment of the watershed being studied.

In the nested watersheds of the Nakanbé River, the transition from the baseline period (1965–1977) to the impacted periods (1978−1994, 1995−2006 and 2007−2018) was characterized by (Fig. 12):

- a continuous degradation, translated by a decrease in the parameter (*w*) value from 1965 to 2018 in the Wayen and Yilou watersheds.
- an improvement of environmental conditions (increase in *w*) from 1965 to 1977 followed by degradation (decrease in *w*) from 1978 to 2018 in the Rambo sub-watershed.
- a degradation (reduction in *w*) from 1965 to 1977 and an improvement from 1995 to 2018 in the Ramsa and Dombré sub-watersheds. In the Ramsa sub-watershed, *w* was relatively stable (between 2.30 and 2.41) due to the opposite environmental dynamics of Rambo and Dombré sub-watersheds it controls.
- a mixed trend in the evolution of *w* in the Tougou and Tempelga sub-watersheds.

Therefore, the evolution of the global environmental parameter (*w*) explains the estimated EC and climate-environment interactions contributions to the runoff change (Table 5). According to the elasticity coefficients found in the nested watersheds of Nakanbé, environmental degradation leads to an increase in runoff, while the increase in *w* leads to runoff decrease. From 1965 to 2018, EC globally contributed positively to the increase in runoff due to environmental degradation. Since 1995, CC has contributed positively to runoff increase due to the precipitation recovery. Over the period 2007−2018, climate-environment interaction has contributed most to the increase in runoff in most watersheds (4 out of 7, as compared to 2 for CC and 1 for EC). From these results, it appears that the first Sahelian hydrological paradox (the runoff increase despite precipitation decrease over 1978−1994) was caused

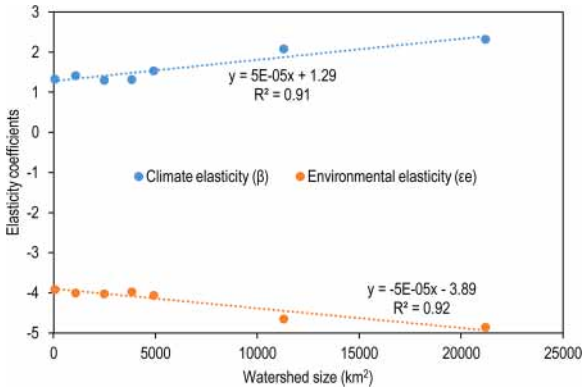

Fig. 11. Evolution of runoff elasticity coefficient to climate change and environmental change with the watershed size.

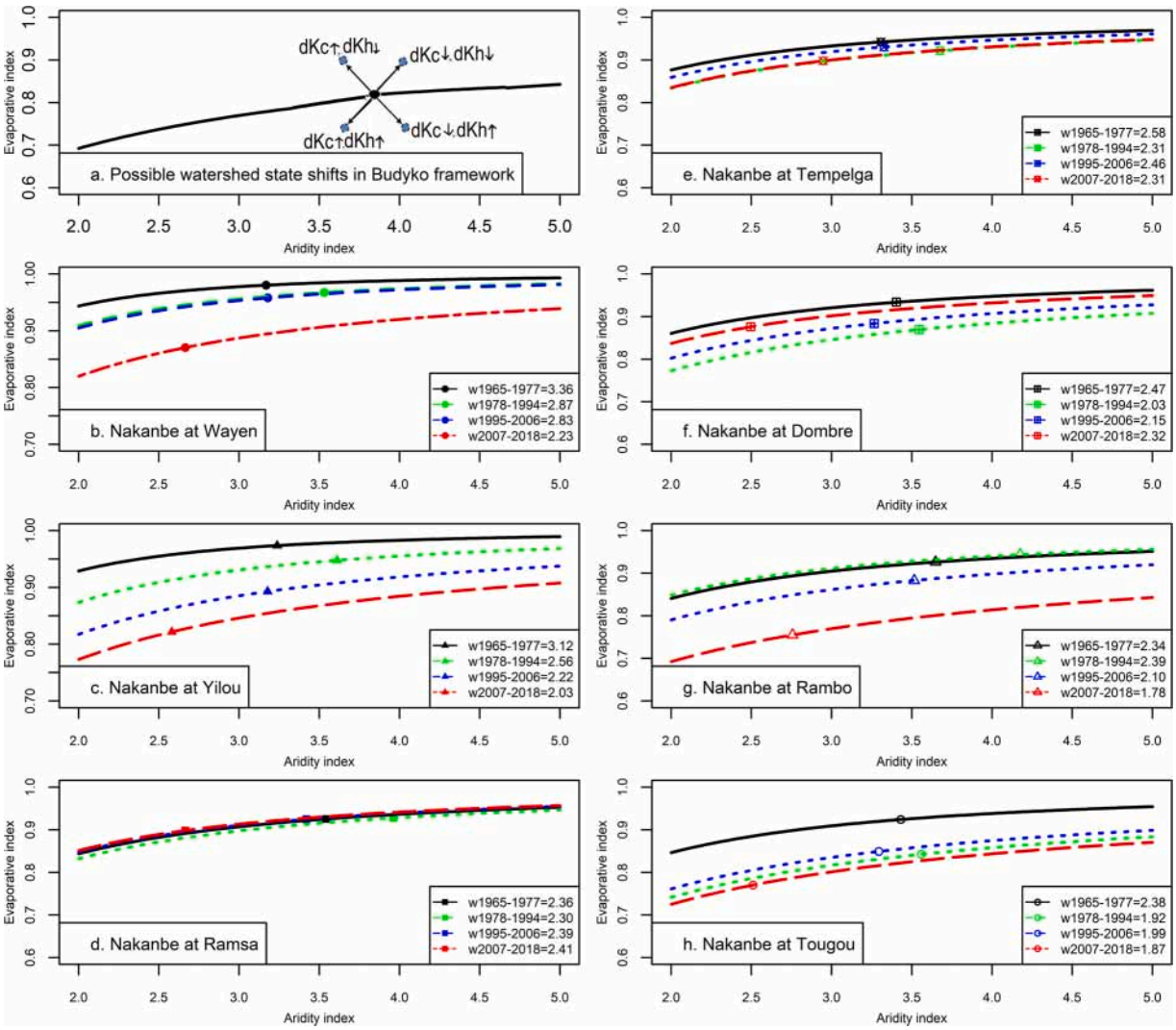

Fig. 12. Evolution of the nested watersheds of Nakanbé in the Budyko framework. In (a) dKc and dKh mean runoff coefficient change due to climate change and human interferences, respectively.

by environmental degradation. In contrast, during the second paradox (increase in runoff coefficients after the precipitation recovery despite the general re-greening), climate-environment interaction was dominant.

4.4. Relationship between the parameter (w) and vegetation coverage (M) in Nakanbé watershed

The seven nested watersheds and 276 grids (8 km × 8 km) were used to look for a link between w and M over the period 1978−1994. Specific-values of w (for watersheds and grids) were obtained by forcing the Budyko model of Fu with aridity and evaporative indexes. Fig. 13 illustrates the spatial variability of the parameter w in the Nakanbé watershed at Wayen. Fig. 14 shows that a linear regression model between w and M is optimal and significant ($R^2 = 0.53$, p_value $< 2.2{\cdot}10^{-16}$) and is given by Eq.(9).

$$w = 6.27 \times M + 0.98 \tag{9}$$

The parameter (w) is positively correlated and proportional to the long-term averaged annual vegetation coverage (M) (Fig. 14), as also found by Li et al. (2013). In the Nakanbé watershed at Wayen, the value $w = 7.25$ was found for dense forests and $w = 0.98$ for completely bare soils, whereas in comparison with Li et al. (2013), these values were $w = 3.52$ for dense forests and $w = 1.16$ for bare soils. The regression slope between w and M in Nakanbé watershed (6.27) is higher than that obtained by Li et al. (2013) (2.36), which means that for the same change in M, the w in Nakanbé watershed will vary by a factor of about 3 from that estimated by the regression model of Li et al. (2013).

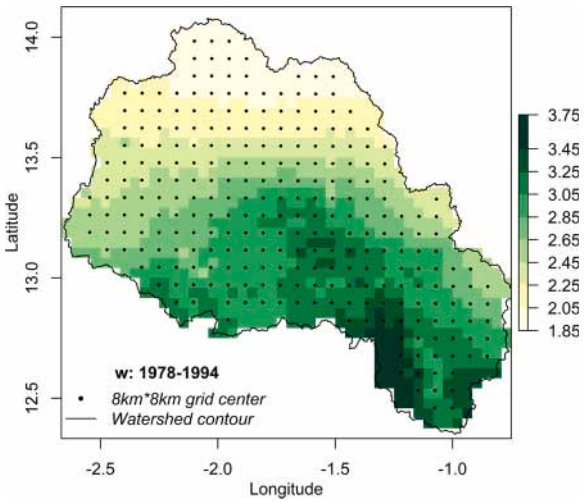

Fig. 13. Spatial variability of the Fu Budyko-type model parameter (w) over the period 1978-1994 in Nakanbé watershed at Wayen.

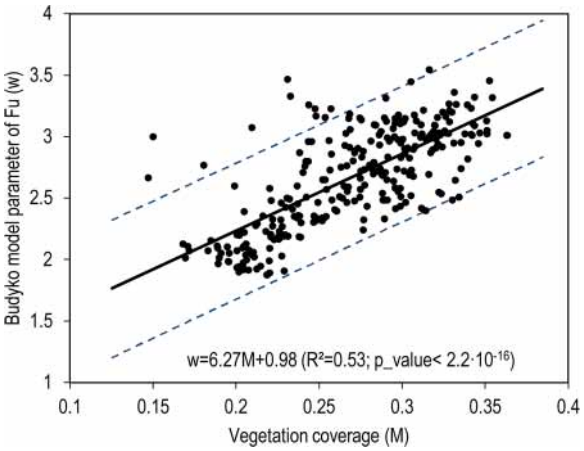

Fig. 14. Relationship between Fu Budyko-type model parameter (*w*) and vegetation coverage (*M*) in Nakanbé watershed at Wayen. The black line represents the linear regression between w and M, blue dashed lines show the 95 % confidence interval around the linear regression model.

5. Discussions and conclusion

5.1. Impact of climate-environment interaction on water resources

In this study, the difference between the total change in runoff and the contribution of climate change (CC) and environmental change (EC) was assumed to be the impact of climate-environment interactions (Eq.(5)). The impacts study showed that (Fig. 10. and Table 5):

- the impact of human interference (*H*) quantified using Budyko curve decomposition is the sum of the impacts of EC and climate-environment interaction,
- Budyko curve decomposition and elasticity methods lead to similar results and,
- from 1978 to 2018, the impact of the climate-environment interaction increased.

Although the impact of climate-environment interaction calculated here could include uncertainties in estimating CC and EC impacts, the values obtained allow us to assume that these uncertainties could not change the observed trends. At a watershed scale, CC can induce EC (Dearing, 2006; Gao et al., 2014). Thus, the impact of climate-environment interaction could be as a result of indirect feedback from the climate: climate influences the environment, which in turn affects the runoff. In the West African Sahel (WAS), the heavy nature of rainfall intensity plays a significant role in forming soil overcrusting, which hampers infiltration and promotes runoff (Ribstein, 1990; Valentin, 1985; Valentin et al., 2004). The increase in soil overcrusting in WAS (Descroix, 2018), likely attributable to

the increase in the intensity of extreme rainfall (Panthou et al., 2018, 2014), would be one of the major causes of the rise in the impact of climate-environment interaction on runoff in Nakanbé watershed at Wayen. Therefore the effect of the climate-environment interaction should be given much attention, as in the face of climate change, rainfall intensity is expected to increase in the WAS (Diedhiou et al., 2018).

5.2. Towards a better understanding of the hydrological behavior of the Nakanbé watershed

The results obtained in this study highlighted that environmental change (EC) was the main driver of runoff change in the nested Nakanbé watersheds at Wayen from 1978 to 1994. However, since 1995, the climate-environment interaction has become increasingly prominent. This result is expected to be the same throughout the West Africa Sahel (WAS) due to the high sensitivity of runoff to EC in arid zones (Fig. 6.a to c). In arid zones ($\varphi > 2$), runoff change is at least twice as sensitive to EC as climate change (CC). These findings quantitatively explain the causes of the two Sahelian hydrological paradoxes (Dardel et al., 2014; Descroix et al., 2018). The impact of precipitation change mainly determines the impact of CC on surface runoff, as the elasticity coefficient of runoff to PE (ε_{PE}) is lower than that of P ($\varepsilon_P = 1 + \mid \varepsilon_{PE} \mid$). The analysis of the spatial variability of the impacts did not reveal any spatial organization. The non-detection of a significant trend between CC and EC contributions and watershed size is undoubtedly due to the size of the watersheds considered, although the relationship between surface runoff and scale is already acknowledged to be complicated in the study area (Mounirou, 2012; Mounirou et al., 2020). Indeed, Pouyaud (1986) proposed that 30,000 km^2 should be considered as a significant 'break surface' in the analysis of the effect of spatial scale of CC and EC on surface runoff in the Volta River watershed in Burkina Faso; while the size of the watersheds in this study ranged from 38 to 21,178 km^2. Below 30,000 km^2, the influence of CC (especially precipitation) is shadowed by that of EC (especially the development of bare soils and crusting, which are predominant in smaller watersheds).

In Budyko-type models, the environmental dynamic is analyzed through the model parameter (w in the Fu equation). As shown by Li et al. (2013), there is a good relationship between the vegetation coverage (M) and w in the Nakanbé watershed at Wayen, but the regression coefficient is higher (Fig. 14). The Nakanbé watershed studied is located in an arid context with high values of w for the same given M in a wet context (Li et al., 2019). The high variation observed between the regression coefficient obtained by Li et al. (2013) and that indicated by this study might be related to the under-representation of arid watersheds in the work of Li et al. (2013) (less than 10 %). It is, therefore, necessary to establish the relationship between w and M for each climatic zone. The relationship obtained in this study is indicative of the Nakanbé watershed at Wayen and it might be necessary to integrate other watersheds before concluding at the full WAS scale.

From 1965 to 2018, the value of parameter w decreased in most of the Nakanbé nested watersheds. This evolution of w is consistent with the downward trend in the soil water holding capacity (WHC) suggested in the Nakanbé River watershed (Diello, 2007; Mahé et al., 2005; Paturel et al., 2017). Furthermore, the factors influencing w and WHC are the same: climate and watershed characteristics (Albergel, 1987; Dunne and Willmott, 1996; Jiang et al., 2015; Li et al., 2013; Mahé et al., 2005; Zhang et al., 2019b). The parameter w can therefore be compared to the WHC of the watershed. In the Dombré sub-watershed, the parameter w increased from 1978 to 2018 despite the increase in the population density (98–156 hbts/km^2 from 1985 to 2006, see Table 4). This observation is at par with the fact that beyond a certain population density, an inverse process of environmental dynamics can be observed (as in the population theory of Boserup): populations are forced to limit the area of cultivated land and to adopt improved agricultural techniques and shift to intensive agriculture geared towards productivity. Indeed, several studies in different African territories showed that the increase in population density can lead to a virtuous agricultural intensification, leading therefore to the improvement of soil fertility and the reduction of soil erosion (and an increase in WHC of soils) (Demont and Jouve, 2000; Descroix, 2018; Luxereau and Roussel, 1997; Planel, 2008; Tiffen et al., 1994). It is worth mentioning the case of M. Yacouba SAWADOGO (Right Livelihood Award 2018), known as the man who stopped the desert (Thor West et al., 2020): between 1980 and 2018; he created a forest (of about 40 ha) from barren and abandoned land in Gourga located in Ouahigouya municipality (in Yatenga province, northern Burkina Faso) in the Dombré sub-watershed area. This result was achieved through the implementation of the soil and water conservation technique called "zaï", which contributes to reducing runoff to promote infiltration, supplying crops and mitigating dry spells (Nyamekye et al., 2018; Zouré et al., 2019). Water harvesting techniques have therefore enabled to increase WHC of the soils in the Dombré sub-watershed. Thus, the parameter w of the Fu model is a good indicator of the spatio-temporal variability of soil WHC in the Sahelian part of the Nakanbé River watershed.

Water holding capacity (WHC) is an essential parameter in most hydrological models. The WHC data available to date are those given in the FAO Soil Map (FAO, 1981; FAO/IIASA/ISRIC/ISS-CAS/JRC, 2012). The FAO Soil map for the WAS is based on soil surveys and information gathered in the 1960s (Nachtergaele et al., 2010) and, therefore, might be outdated. The use of time-varying values of soil WHC can improve the performance of hydrological model applications in the WAS watersheds (Diello, 2007; Mahé et al., 2005; Paturel et al., 2017). In the light of this study results, the parameter w can therefore be used to provide time-varying soil WHC to this end.

According to the elasticity coefficient of runoff to environmental change (Table 5), the relationship between vegetation coverage (M) and the parameter (w) in the watershed of Nakanbé at Wayen (Eq.(9)), an increase in vegetation coverage (M) would lead to an increase in w by order of 1.45–1.80 and a decrease of runoff by order of 2.43 to 3.36. Therefore, the adoption of an adequate environmental management policy to promote environmental restoration might help in mitigating the increase in runoff coefficient, which is reported to be the cause of significant flooding events throughout the WAS (Coulibaly et al., 2020; Nka et al., 2015; Sighomnou et al., 2013; Tazen et al., 2019).

6. Conclusion

This study focused on seven nested watersheds located in the Sahel part of Nakanbé River in Burkina Faso. It aimed to identify a suitable Budyko-type model for arid contexts, such as in West Africa Sahel (WAS) and to analyze the impacts of climate change (CC), environmental change (EC) and climate-environment interaction on water resources in Nakanbé watershed at Wayen. The Budyko-type model of Fu was found to be appropriate through a sensitivity analysis. Therefore, the isolated and combined impacts of CC and EC on runoff change were quantified based on elasticity and Budyko curve decomposition methods. From these results, the evolution of the hydrological behavior of Nakanbé watershed at Wayen was assessed through the analysis of the spatio-temporal variability of the parameter *w* (from the Fu model) and its relationship with the vegetation coverage (*M*).

Our results confirmed that the Nakanbé watershed at Wayen had undergone the two Sahelian hydrological paradoxes. From 1965 to 2018, the runoff coefficient increased: the runoff coefficient over the period 2007–2014 became 4 times higher than that of the period 1965–1977. The environmental conditions of the watershed area are characterized by low vegetation coverage, albeit presenting a substantial variability. The impact studies showed that elasticity and Budyko curve decomposition methods gave similar results ($R^2 = 0.99$). The impact of human interferences quantified by the decomposition method includes the impacts of EC and climate-environment interactions. From 1978 to 1994, EC had been the main driver of runoff change in the Nakanbé nested watersheds (contribution reached 175 %), but climate-environment interaction became increasingly predominant (contribution reached 68 % over the period 2007−2018). The analysis of the variability of the impacts did not reveal a significant trend between CC/EC contributions and watershed size. However, in the Nakanbé watershed at Wayen, there is a good and consistent relationship between the vegetation coverage (*M*) and the parameter *w*. From 1965 to 2018, *w* decreased in all watersheds except in that of Dombré, possibly due to the long-term implementation of water-harvesting techniques, which is effective in the increase of the soil water holding capacity (WHC). Therefore, *w* appears to be a good indicator of the spatio-temporal variability of the soils WHC, which could be used to generate time-varying values of WHC to improve the performance of hydrological models.

Author contributions

Y. Patrick Gbohoui: Conceptualization, Methodology, Formal analysis, Writing; **Jean-Emmanuel Paturel:** Conceptualization, Methodology, Writing – Review, Supervision; **Fowe Tazen:** Conceptualization, Methodology, Writing – Review; **Lawani A. Mounirou and Roland Yonaba**: Writing – Review; **Harouna Karambiri and Hamma Yacouba:** Supervision and Project administration.

Funding

This research was carried out within the framework of the Project « Nelson Mandela Institutes-African Institutions of Science and Technology », supported by the African Development Bank [Project n°:P-Z1-IA0−013, Grant n°:2100155032824].

Declaration of Competing Interest

The authors declare that they have no known competing financial interests or personal relationships that could have appeared to influence the work reported in this paper.

Acknowledgments

The authors wish to thank all people who contributed to this work by reading or giving wise advice.

Appendix A. Derivation of the Budyko framework for obtaining the expressions of climate and environmental elasticity as well as the impacts of climate change, environmental change and climate-environment interaction

According to Eq.(3), the conceptual framework of Budyko can be rewritten in Eq. (A1):

$$\begin{cases} \dfrac{AE}{P} = f(\varphi, e) \\ \varphi = \dfrac{PE}{P} \end{cases} \tag{A1}$$

where AE, P and PE are, respectively, the annual average of actual evapotranspiration, precipitation and potential evapotranspiration over the study period. φ is the aridity index, e the parameter which considers the environmental dynamic and f the Budyko function.

Assuming negligible in the long-term changes in subsurface water storage and net heat transfer between the land surface and the vadose zone, we have:

$$\begin{cases} AE = P - R \\ R = P[1 - f(\varphi, e)] \end{cases} \tag{A2}$$

where R is the annual average of runoff over the study period

By omitting the interactions between P, PE and e, we can write:

$$\begin{cases} dR = \dfrac{\partial R}{\partial P}dP + \dfrac{\partial R}{\partial PE}dPE + \dfrac{\partial R}{\partial e}de \\ \dfrac{dR}{dP} = \dfrac{\partial R}{\partial P} = 1 - f(\varphi, e) - P\dfrac{\partial f}{\partial \varphi}\dfrac{\partial \varphi}{\partial P} = 1 - f(\varphi, e) + \varphi\dfrac{\partial f}{\partial \varphi}, because \dfrac{\partial \varphi}{\partial P} = -\dfrac{\varphi}{P} \\ \dfrac{dR}{dPE} = \dfrac{\partial R}{\partial PE} = -P\dfrac{\partial f}{\partial \varphi}\dfrac{\partial \varphi}{\partial PE} = -\dfrac{\varphi \partial f}{\partial \varphi}, because \dfrac{\partial \varphi}{\partial PE} = \dfrac{1}{P} \\ \dfrac{\partial R}{\partial e} = -P\dfrac{\partial f}{\partial e} \end{cases} \tag{A3}$$

By integrating the expressions of the partial derivatives into that of the complete derivative of R and after readjustments, we obtain the expressions of climate and environment elasticities as well as those of the contributions of climate, environment and climate-environment interaction to the runoff change (Eq. A4):

$$\begin{cases} dR = \dfrac{1 - f(\varphi, e) + \varphi\dfrac{\partial f}{\partial \varphi}}{P[1 - f(\varphi, e)]}RdP + \dfrac{-\dfrac{\partial f}{\partial \varphi}}{P[1 - f(\varphi, e)]}RdPE + \dfrac{-P\dfrac{\partial f}{\partial e}}{P[1 - f(\varphi, e)]}Rde \\ dR = R\left[1 + \dfrac{\varphi\dfrac{\partial f}{\partial \varphi}}{1 - f(\varphi, e)}\right]\dfrac{dP}{P} - R\dfrac{\dfrac{\partial f}{\partial \varphi}}{1 - f(\varphi, e)}\dfrac{dPE}{\dfrac{PE}{\varphi}} - R\dfrac{e\dfrac{\partial f}{\partial e}}{1 - f(\varphi, e)}\dfrac{de}{e} \\ dR = \left[(1 + \beta)\dfrac{dP}{P} - \beta\dfrac{dPE}{PE}\right]R + \varepsilon_e\dfrac{de}{e}R; \beta = \dfrac{\varphi}{1 - f(\varphi, e)}\dfrac{\partial f}{\partial \varphi}et\varepsilon_e = \dfrac{-e}{1 - f(\varphi, e)}\dfrac{\partial f}{\partial e} \\ \Delta R = \left[(1 + \beta)\dfrac{\Delta P}{P} - \beta\dfrac{\Delta PE}{PE}\right]R + \varepsilon_e\dfrac{\Delta e}{e}R \\ C_C = \left[(1 + \beta)\dfrac{\Delta P}{P} - \beta\dfrac{\Delta PE}{PE}\right]\dfrac{R}{\Delta R} \\ C_E = \varepsilon_e\dfrac{\Delta e}{e}\dfrac{R}{\Delta R} \\ C_{ICE} = 1 - C_c - C_e \end{cases} \tag{A4}$$

β and ε_e are related to the elasticities of the climate and the environment, respectively. C_C, C_E and C_{ICE} are the respective contributions of climate change, environmental change and climate-environment interaction to runoff change.

Appendix B. Supplementary data

Supplementary material related to this article can be found, in the online version, at doi:https://doi.org/10.1016/j.ejrh.2021.100828.

References

Abatzoglou, J.T., Dobrowski, S.Z., Parks, S.A., Hegewisch, K.C., 2018. Terra Climate, a high-resolution global dataset of monthly climate and climatic water balance from 1958–2015. Sci. Data. https://doi.org/10.7923/G43J3B0R [dataset].

Albergel, J., 1987. Genèse Et Prédétermination Des Crues Au Burkina Faso. Etudes Thèses. ORSTOM, Paris.

ALOS, 2020. Global Digital Surface Model "ALOS World 3D - 30m" (AW3D30) [dataset]. https://www.eorc.jaxa.jp/ALOS/en/aw3d30/index.htm.

Arora, V.K., 2002. The use of the aridity index to assess climate change effect on annual runoff. J. Hydrol. 265, 164–177. https://doi.org/10.1016/S0022-1694(02)00101-4.

Bai, M., Shen, B., Song, X., Mo, S., Huang, L., Quan, Q., 2019. Multi-temporal variabilities of evapotranspiration rates and their associations with climate change and vegetation greening in the Gan River Basin. China. Water 11, 2568. https://doi.org/10.3390/w11122568.

Beck, H.E., Wood, E.F., Pan, M., Fisher, C.K., Miralles, D.G., van Dijk, A.I.J.M., McVicar, T.R., Adler, R.F., 2019. MSWEP V2 global 3-Hourly 0.1° precipitation: methodology and quantitative assessment. Bull. Am. Meteorol. Soc. [dataset] http://www.gloh2o.org/.

Blöschl, G., Ardoin-Bardin, S., Bonell, M., Dorninger, M., Goodrich, D., Gutknecht, D., Matamoros, D., Merz, B., Shand, P., Szolgay, J., 2007. At what scales do climate variability and land cover change impact on flooding and low flows? Hydrol. Process. 21, 1241–1247. https://doi.org/10.1002/hyp.6669.

Blöschl, G., Sivapalan, M., Wagener, T., Savenije, H., Viglione, A., 2013. Runoff Prediction in Ungauged Basins: Synthesis across Processes, Places and Scales. Cambridge University Press.

Boyer, J.-F., Dieulin, C., Rouche, N., Cres, A., Servat, E., Paturel, J.-E., Mahé, G., 2006. SIEREM: an environmental information system for water resources. IAHS Publ. [dataset] http://www.hydrosciences.fr/SIEREM/.

Budyko, M.I., 1974. Climate and Life. Academic Press, New York.

Casenave, A., Valentin, C., 1991. Influence des etats de surface sur l'infiltration en zone sahelienne. IAHS Publ 89–108.

Choudhury, B.J., 1999. Evaluation of an empirical equation for annual evaporation using field observations and results from a biophysical model. J. Hydrol. 216, 99–110.
Coulibaly, G., Leye, B., Tazen, F., Mounirou, L.A., Karambiri, H., 2020. Urban flood modeling using 2D shallow-water equations in Ouagadougou, burkina faso. Water 12, 2120. https://doi.org/10.3390/w12082120.
Dardel, C., Kergoat, L., Hiernaux, P., Grippa, M., Mougin, E., Ciais, P., Nguyen, C.-C., 2014. Rain-use-Efficiency: what it tells us about the conflicting sahel greening and sahelian paradox. Remote Sens. 6, 3446–3474. https://doi.org/10.3390/rs6043446.
De Longueville, F., Hountondji, Y.-C., Kindo, I., Gemenne, F., Ozer, P., 2016. Long-term analysis of rainfall and temperature data in Burkina Faso (1950-2013). Int. J. Climatol. 36, 4393–4405. https://doi.org/10.1002/joc.4640.
Dearing, J.A., 2006. Climate-human-environment Interactions: Resolving Our Past.
Dembélé, M., Schaefli, B., van de Giesen, N., Mariéthoz, G., 2020. Suitability of 17 rainfall and temperature gridded datasets for largescale hydrological modelling in West Africa. Hydrol. Earth Syst. Sci. Discuss. 1–39. https://doi.org/10.5194/hess-2020-68.
Dembélé, M., Zwart, S.J., 2016. Evaluation and comparison of satellite-based rainfall products in Burkina Faso, West Africa. Int. J. Remote Sens. 37, 3995–4014. https://doi.org/10.1080/01431161.2016.1207258.
Demont, M., Jouve, P., 2000. Evolution d'agro-écosystèmes Villageois Dans La Région De Korhogo (Nord Côte d'Ivoire): Borserup Versus Malthus, Opposition Ou Complémentarité? Presented at the Dynamiques Agraires Et Construction Sociale Du Territoire. CNEARC, pp. 93–108.
Descroix, L., 2018. Processus Et Enjeux d'eau En Afrique De l'Ouest Soudano-sahélienne. Archives contemporaines.
Descroix, L., Mahé, G., Lebel, T., Favreau, G., Galle, S., Gautier, E., Olivry, J., Albergel, J., Amogu, O., Cappelaere, B., et al., 2009. Spatio-temporal variability of hydrological regimes around the boundaries between Sahelian and Sudanian areas of West Africa: a synthesis. J. Hydrol. 375, 90–102. https://doi.org/10.1016/j.jhydrol.2008.12.012.
Descroix, L., Guichard, F., Grippa, M., Lambert, L., Panthou, G., Mahé, G., Gal, L., Dardel, C., Quantin, G., Kergoat, L., Bouaïta, Y., Hiernaux, P., Vischel, T., Pellarin, T., Faty, B., Wilcox, C., Malam Abdou, M., Mamadou, I., Vandervaere, J.-P., Diongue-Niang, A., Ndiaye, O., Sané, Y., Dacosta, H., Gosset, M., Cassé, C., Sultan, B., Barry, Aliou, Amogu, O., Nka Nnomo, B., Barry, Alseny, Paturel, J.-E., 2018. Evolution of surface hydrology in the sahelo-sudanian strip: an updated review. Water 10, 748. https://doi.org/10.3390/w10060748.
Dey, P., Mishra, A., 2017. Separating the impacts of climate change and human activities on streamflow: a review of methodologies and critical assumptions. J. Hydrol. 548, 278–290. https://doi.org/10.1016/j.jhydrol.2017.03.014.
Diedhiou, A., Bichet, A., Wartenburger, R., Seneviratne, S.I., Rowell, D.P., Sylla, M.B., Diallo, I., Todzo, S., N' datchoh, E.T., Camara, M., et al., 2018. Changes in climate extremes over West and Central Africa at 1.5 C and 2 C global warming. Environ. Res. Lett. 13, 065020 https://doi.org/10.1088/1748-9326/aac3e5.
Diello, P., 2007. Interrelations Climat – Homme – Environnement Dans Le Sahel Burkinabé: Impacts Sur Les États De Surface Et La Modélisation Hydrologique. Ph.D. Thesis. Montpellier 2-IRD/ 2iE, France/Burkina Faso.
Donohue, R.J., Roderick, M.L., McVicar, T.R., 2011. Assessing the differences in sensitivities of runoff to changes in climatic conditions across a large basin. J. Hydrol. 406, 234–244. https://doi.org/10.1016/j.jhydrol.2011.07.003.
Dooge, J.C., 1992. Sensitivity of runoff to climate change: a Hortonian approach. Bull. Am. Meteorol. Soc. 73, 2013–2024.
Du, C., Sun, F., Yu, J., Liu, X., Chen, Y., 2016. New interpretation of the role of water balance in an extended Budyko hypothesis in arid regions. Hydrol. Earth Syst. Sci. 20, 393–409. https://doi.org/10.5194/hess-20-393-2016.
Dunne, K., Willmott, C.J., 1996. Global distribution of plant-extractable water capacity of soil. Int. J. Climatol. J. R. Meteorol. Soc. 16, 841–859. https://doi.org/10.1002/(SICI)1097-0088(199608)16:8<841::AID-JOC60>3.0.CO;2-8.
FAO, 1981. Digital Soil Map of the World. UNESCO [dataset].
FAO/IIASA/ISRIC/ISS-CAS/JRC, 2012. Harmonized World Soil Database (version 1.2). FAO, Rome, Italy and IIASA, Laxenburg, Austria [dataset].
Fathi, M.M., Awadallah, A.G., Abdelbaki, A.M., Haggag, M., 2019. A new Budyko framework extension using time series SARIMAX model. J. Hydrol. 570, 827–838. https://doi.org/10.1016/j.jhydrol.2019.01.037.
Fu, B., 1981. On the calculation of the evaporation from land surface. Sci Atmos Sin 5, 23–31.
Funk, C.C., Peterson, P.J., Landsfeld, M.F., Pedreros, D.H., Verdin, J.P., Rowland, J.D., Romero, B.E., Husak, G.J., Michaelsen, J.C., Verdin, A.P., 2014. A Quasi-Global Precipitation Time Series for Drought Monitoring: U.S. Geological Survey Data Series, 832, p. 4 [dataset] https://doi.org/110.3133/ds832.
Gal, L., Grippa, M., Hiernaux, P., Pons, L., Kergoat, L., 2017. The paradoxical evolution of runoff in the pastoral Sahel: analysis of the hydrological changes over the Agoufou watershed (Mali) using the KINEROS-2 model. Hydrol. Earth Syst. Sci. 21, 4591–4613. https://doi.org/10.5194/hess-21-4591-2017.
Gao, H., Hrachowitz, M., Schymanski, S., Fenicia, F., Sriwongsitanon, N., Savenije, H., 2014. Climate controls how ecosystems size the root zone storage capacity at catchment scale. Geophys. Res. Lett. 41, 7916–7923. https://doi.org/10.1002/2014GL061668.
Greve, P., Gudmundsson, L., Orlowsky, B., Seneviratne, S.I., 2016. A two-parameter Budyko function to represent conditions under which evapotranspiration exceeds precipitation. Hydrol. Earth Syst. Sci. 20, 2195–2205. https://doi.org/10.5194/hess-20-2195-2016.
Grijsen, J., Brown, C., Tarhule, A., Ghile, Y., Taner, Ü., Talbi-Jordan, A., Doffou, H., Guero, A., Dessouassi, R., Kone, S., et al., 2013. Climate risk assessment for water resources development in the Niger River basin part I: context and climate projections. Climate Variability-Regional and Thematic Patterns. IntechOpen.
Guo, L., Shan, N., Zhang, Y., Sun, F., Liu, W., Shi, Z., Zhang, Q., 2019. Separating the effects of climate change and human activity on water use efficiency over the Beijing-Tianjin Sand Source Region of China. Sci. Total Environ. 690, 584–595. https://doi.org/10.1016/j.scitotenv.2019.07.067.
Gupta, H.V., Kling, H., Yilmaz, K.K., Martinez, G.F., 2009. Decomposition of the mean squared error and NSE performance criteria: implications for improving hydrological modelling. J. Hydrol. 377, 80–91. https://doi.org/10.1016/j.jhydrol.2009.08.003.
Harman, C., Troch, P.A., 2014. What makes Darwinian hydrology" Darwinian"? Asking a different kind of question about landscapes. Hydrol. Earth Syst. Sci. 18, 417. https://doi.org/10.5194/hess-18-417-2014.
Hasan, E., Tarhule, A., Kirstetter, P.-E., Clark III, R., Hong, Y., 2018. Runoff sensitivity to climate change in the Nile River Basin. J. Hydrol. 561, 312–321. https://doi.org/10.1016/j.jhydrol.2018.04.004.
Hubert, P., Carbonnel, J.P., Chaouche, A., 1989. Segmentation des séries hydrométéorologiques — application à des séries de précipitations et de débits de l'afrique de l'ouest. J. Hydrol. 110, 349–367. https://doi.org/10.1016/0022-1694(89)90197-2.
Ibrahim, B., 2012. Caractérisation Des Saisons De Pluies Au Burkina Faso Dans Un Contexte De Changement Climatique Et Évaluation Des Impacts Hydrologiques Sur Le Bassin Du Nakanbé. PhD Thesis. 2iE et Université Pierre et Marie Curie, Ouagadougou et Paris VI.
Jiang, C., Xiong, L., Wang, D., Liu, P., Guo, S., Xu, C.-Y., 2015. Separating the impacts of climate change and human activities on runoff using the Budyko-type equations with time-varying parameters. J. Hydrol. 522, 326–338. https://doi.org/10.1016/j.jhydrol.2014.12.060.
Kang, Y., Gao, J., Shao, H., Zhang, Y., 2020. Quantitative analysis of hydrological responses to climate variability and land-use change in the hilly-gully region of the Loess Plateau, China. Water 12, 82. https://doi.org/10.3390/w12010082.
Karambiri, H., García Galiano, S.G., Giraldo, J.D., Yacouba, H., Ibrahim, B., Barbier, B., Polcher, J., 2011. Assessing the impact of climate variability and climate change on runoff in West Africa: the case of Senegal and Nakambe River basins. Atmospheric Sci. Lett. 12, 109–115. https://doi.org/10.1002/asl.317.
Kundzewicz, Z.W., Graczyk, D., Maurer, T., Pińskwar, I., Radziejewski, M., Svensson, C., Szwed, M., 2005. Trend detection in river flow series: 1. Annual maximum flow/Détection de tendance dans des séries de débit fluvial: 1. Débit maximum annuel. Hydrol. Sci. J. 50.
Lebel, T., Ali, A., 2009. Recent trends in the Central and Western Sahel rainfall regime (1990–2007). J. Hydrol. 375, 52–64. https://doi.org/10.1016/j.jhydrol.2008.11.030.
Li, D., Pan, M., Cong, Z., Zhang, L., Wood, E., 2013. Vegetation control on water and energy balance within the Budyko framework. Water Resour. Res. 49, 969–976. https://doi.org/10.1002/wrcr.20107.
Li, Y., Liu, C., Yu, W., Tian, D., Bai, P., 2019. Response of streamflow to environmental changes: a Budyko-type analysis based on 144 river basins over China. Sci. Total Environ. 664, 824–833. https://doi.org/10.1016/j.scitotenv.2019.02.011.
Liu, N., Harper, R., Smettem, K., Dell, B., Liu, S., 2019. Responses of streamflow to vegetation and climate change in southwestern Australia. J. Hydrol. 572, 761–770. https://doi.org/10.1016/j.jhydrol.2019.03.005.

Luxereau, A., Roussel, B., 1997. Changements Écologiques Et Sociaux Au Niger: Des Interactions Étroites.
Mahé, G., 2006. Variabilité pluie-débit en Afrique de l'Ouest et Centrale au 20ème siècle: changements hydro-climatiques, occupation du sol et modélisation hydrologique. Univ. Montp. II Montp. Fr. 2, 160.
Mahé, G., Paturel, J.-E., 2009. 1896–2006 Sahelian annual rainfall variability and runoff increase of Sahelian Rivers. Comptes Rendus Geosci. 341, 538–546. https://doi.org/10.1016/j.crte.2009.05.002.
Mahé, G., Paturel, J.-E., Servat, E., Conway, D., Dezetter, A., 2005. The impact of land use change on soil water holding capacity and river flow modelling in the Nakambe River, Burkina-Faso. J. Hydrol. 300, 33–43. https://doi.org/10.1016/j.jhydrol.2004.04.028.
Mangini, W., Viglione, A., Hall, J., Hundecha, Y., Ceola, S., Montanari, A., Rogger, M., Salinas, J.L., Borzì, I., Parajka, J., 2018. Detection of trends in magnitude and frequency of flood peaks across Europe. Hydrol. Sci. J. 63, 493–512. https://doi.org/10.1080/02626667.2018.1444766.
Mango, L.M., Melesse, A.M., McClain, M.E., Gann, D., Setegn, S.G., 2011. Land use and climate change impacts on the hydrology of the upper Mara river Basin, Kenya: results of a modeling study to support better resource management. Hydrol. Earth Syst. Sci. 15, 2245–2258. https://doi.org/10.5194/hess-15-2245-2011.
McCuen, R.H., 1974. A sensitivity and error analysis CF procedures used for estimating evaporation 1. JAWRA J. Am. Water Resour. Assoc. 10, 486–497. https://doi.org/10.1111/j.1752-1688.1974.tb00590.x.
McVicar, T.R., Roderick, M.L., Donohue, R.J., Van Niel, T.G., 2012. Less bluster ahead? Ecohydrological implications of global trends of terrestrial near-surface wind speeds. Ecohydrology 5, 381–388. https://doi.org/10.1002/eco.1298.
Moriasi, D.N., Arnold, J.G., Van Liew, M.W., Bingner, R.L., Harmel, R.D., Veith, T.L., 2007. Model evaluation guidelines for systematic quantification of accuracy in watershed simulations. Trans. ASABE 50, 885–900. https://doi.org/10.13031/2013.23153.
Mounirou, L.A., 2012. Etude Du Ruissellement Et De l'érosion à Différentes Échelles Spatiales Sur Le Bassin Versant De Tougou En Zone Sahélienne Du Burkina Faso: Quantification Et Transposition Des Données. PhD Thesis. Montpellier 2-2iE, Burkina-Faso.
Mounirou, L.A., Zouré, C.O., Yonaba, R., Paturel, J.-E., Mahé, G., Niang, D., Yacouba, H., Karambiri, H., 2020. Multi-scale analysis of runoff from a statistical perspective in a small Sahelian catchment under semi-arid climate. Arab. J. Geosci. 13, 154. https://doi.org/10.1007/s12517-020-5141-2.
Nachtergaele, F., van Velthuizen, H., Verelst, L., Batjes, N., Dijkshoorn, K., van Engelen, V., Fischer, G., Jones, A., Montanarela, L., 2010. The harmonized world soil database. In: Proceedings of the 19th World Congress of Soil Science, Soil Solutions for a Changing World. Brisbane, Australia, 1-6 August 2010, pp. 34–37.
National Center for Atmospheric Research Staff (Ed.), 2018. NDVI: Normalized Difference Vegetation Index-3rd Generation. NASA/GFSC GIMMS | NCAR. - Climate Data Guide. https://climatedataguide.ucar.edu/climate-data/ndvi-normalized-difference-vegetation-index-3rd-generation-nasagfsc-gimms [dataset].
Ning, T., Zhou, S., Chang, F., Shen, H., Li, Z., Liu, W., 2019. Interaction of vegetation, climate and topography on evapotranspiration modelling at different time scales within the Budyko framework. Agric. For. Meteorol. 275, 59–68. https://doi.org/10.1016/j.agrformet.2019.05.001.
Nka, B.N., Oudin, L., Karambiri, H., Paturel, J.E., Ribstein, P., 2015. Trends in floods in West Africa: analysis based on 11 catchments in the region. Hydrol. Earth Syst. Sci. 19, 4707–4719. https://doi.org/10.5194/hess-19-4707-2015.
Novella, N.S., Thiaw, W.M., 2012. African rainfall climatology version 2 for famine early warning systems. J. Appl. Meteorol. Climatol. [dataset] https://iridl.ldeo.columbia.edu/SOURCES/.NOAA/.NCEP/.CPC/.FEWS/.Africa/.DAILY/.ARC2/.daily/.
Nyamekye, C., Thiel, M., Schönbrodt-Stitt, S., Zoungrana, B.J.-B., Amekudzi, L.K., 2018. Soil and water conservation in Burkina Faso, West Africa. Sustainability 10, 3182. https://doi.org/10.3390/su10093182.
Olawoyin, R., Acheampong, P.K., 2017. Objective assessment of the Thiessen polygon method for estimating areal rainfall depths in the River Volta catchment in Ghana. Ghana J. Geogr. 9, 151–174. https://doi.org/10.4314/gjg.v9i2.
Panthou, G., Vischel, T., Lebel, T., 2014. Recent trends in the regime of extreme rainfall in the central Sahel: recent trends of extreme rainfall in the West African Sahel. Int. J. Climatol. 34, 3998–4006. https://doi.org/10.1002/joc.3984.
Panthou, G., Lebel, T., Vischel, T., Quantin, G., Sane, Y., Ba, A., Ndiaye, O., Diongue-Niang, A., Diopkane, M., 2018. Rainfall intensification in tropical semi-arid regions: the Sahelian case. Environ. Res. Lett. 13, 064013 https://doi.org/10.1088/1748-9326/aac334.
Paturel, J.-E., Ouedraogo, M., Servat, E., Mahé, G., Dezetter, A., Boyer, J.-F., 2003. The concept of rainfall and streamflow normals in West and Central Africa in a context of climatic variability. Hydrol. Sci. J. 48, 125–137. https://doi.org/10.1623/hysj.48.1.125.43479.
Paturel, J.E., Mahé, G., Diello, P., Barbier, B., Dezetter, A., Dieulin, C., Karambiri, H., Yacouba, H., Maiga, A., 2017. Using land cover changes and demographic data to improve hydrological modeling in the Sahel: improving hydrological modelling in the Sahel. Hydrol. Process. 31, 811–824. https://doi.org/10.1002/hyp.11057.
Pellarin, T., Louvet, S., Gruhier, C., Quantin, G., Legout, C., 2013. A simple and effective method for correcting soil moisture and precipitation estimates using AMSR-E measurements. Remote Sens. Environ. 136, 28–36. https://doi.org/10.1016/j.rse.2013.04.011.
Peng, S., Liu, W., Wang, W., Shao, Q., Jiao, X., Yu, Z., Xing, W., Xu, J., Zhang, Z., Luo, Y., 2013. Estimating the effects of climatic variability and human activities on streamflow in the Hutuo River Basin, China. J. Hydrol. Eng. 18, 422–430. https://doi.org/10.1061/(ASCE)HE.1943-5584.0000664.
Pettitt, A.N., 1979. A non-parametric approach to the change-point problem. Appl. Stat. 28, 126. https://doi.org/10.2307/2346729.
Piemontese, L., Fetzer, I., Rockström, J., Jaramillo, F., 2019. Future hydroclimatic impacts on Africa: beyond the Paris agreement. Earths Future 7, 748–761. https://doi.org/10.1029/2019EF001169.
Pinzon, J.E., Tucker, C.J., 2014. A non-stationary 1981–2012 AVHRR NDVI3g time series. Remote Sens. 6, 6929–6960. https://doi.org/10.3390/rs6086929.
Planel, S., 2008. La Chute d' Un Éden Éthiopien: Le Wolaita, Une Campagne En Recomposition. IRD Editions.
Porporato, A., Daly, E., Rodriguez-Iturbe, I., 2004. Soil water balance and ecosystem response to climate change. Am. Nat. 164, 625–632.
Pouyaud, B., 1986. Estimation Des Apports Annuels Et Des Étiages, Avant Et Après La Récente Phase De Sécheresse, De La Volta Noire à Noumbiel Et De La Volta Blanche à Bagré.
Ribstein, P., 1990. Modèles De Crues Et Petits Bassins Versants Au Sahel (Thèse De Doctorat). Univ. Sc. et Tech. du Languedoc, Montpellier.
Robson, A.J., 2002. Evidence for trends in UK flooding. Philos. Trans. R. Soc. Math. Phys. Eng. Sci. 360, 1327–1343. https://doi.org/10.1098/rsta.2002.1003.
Sighomnou, D., Descroix, L., Genthon, P., Mahé, G., Moussa, I.B., Gautier, E., Mamadou, I., Vandervaere, J.-P., Bachir, T., Coulibaly, B., et al., 2013. The Niger River Niamey flood of 2012: The paroxysm of the Sahelian paradox? Sci. Chang. PlanétairesSécheresse 24, 3–13. https://doi.org/10.1684/sec.2013.0370.
Sivapalan, M., Blöschl, G., Zhang, L., Vertessy, R., 2003. Downward approach to hydrological prediction. Hydrol. Process. 17, 2101–2111. https://doi.org/10.1002/hyp.1425.
Sposito, G., 2017. Understanding the budyko equation. Water 9, 236. https://doi.org/10.3390/w9040236.
Svensson, C., Kundzewicz, W.Z., Maurer, T., 2005. Trend detection in river flow series: 2. Flood and low-flow index series/Détection de tendance dans des séries de débit fluvial: 2. Séries d'indices de crue et d'étiage. Hydrol. Sci. J. 50.
Taylor, C.M., Gounou, A., Guichard, F., Harris, P.P., Ellis, R.J., Couvreux, F., De Kauwe, M., 2011. Frequency of Sahelian storm initiation enhanced over mesoscale soil-moisture patterns. Nat. Geosci. 4, 430–433.
Tazen, F., Diarra, A., Kabore, R.F., Ibrahim, B., Bologo/Traoré, M., Traoré, K., Karambiri, H., 2019. Trends in flood events and their relationship to extreme rainfall in an urban area of Sahelian West Africa: the case study of Ouagadougou, Burkina Faso. J. Flood Risk Manag. 12, e12507 https://doi.org/10.1111/jfr3.12507.
Teuling, A.J., de Badts, E.A.G., Jansen, F.A., Fuchs, R., Buitink, J., Hoek van Dijke, A.J., Sterling, S.M., 2019. Climate change, reforestation/afforestation and urbanization impacts on evapotranspiration and streamflow in Europe. Hydrol. Earth Syst. Sci. 23, 3631–3652. https://doi.org/10.5194/hess-23-3631-2019.
Thor West, C., Benecky, S., Karlsson, C., Reiss, B., Moody, A.J., 2020. Bottom-up perspectives on the Re-Greening of the sahel: an evaluation of the spatial relationship between soil and water conservation (SWC) and tree-cover in Burkina Faso. Land 9, 208. https://doi.org/10.3390/land9060208.
Tiffen, M., Mortimore, M., Gichuki, F., et al., 1994. More People, Less Erosion: Environmental Recovery in Kenya. John Wiley & Sons Ltd.
Tomer, M.D., Schilling, K.E., 2009. A simple approach to distinguish land-use and climate-change effects on watershed hydrology. J. Hydrol. 376, 24–33. https://doi.org/10.1016/j.jhydrol.2009.07.029.
University Of East Anglia Climatic Research Unit (CRU), Harris, I.C., Jones, P.D., 2020. CRU TS Version 4.03. Cent. Environ. Data Anal. CEDA [dataset]. https://crudata.uea.ac.uk/cru/data/hrg/cru_ts_4.03/.

Valentin, C., 1985. Organisations Pelliculaires Superficielles De Quelques Sols De Région Subdésertique. AGADEZ-République du Niger. Thèse, Etudes et Thèses ORSTOM. ed.
Valentin, C., Rajot, J.-L., Mitja, D., 2004. Responses of soil crusting, runoff and erosion to fallowing in the sub-humid and semi-arid regions of West Africa. Agric. Ecosyst. Environ. 104, 287–302. https://doi.org/10.1016/j.agee.2004.01.035.
Wang, D., Hejazi, M., 2011. Quantifying the relative contribution of the climate and direct human impacts on mean annual streamflow in the contiguous United States. Water Resour. Res. 47 https://doi.org/10.1029/2010WR010283.
Wang, D., Tang, Y., 2014. A one-parameter Budyko model for water balance captures emergent behavior in Darwinian hydrologic models. Geophys. Res. Lett. 41, 4569–4577. https://doi.org/10.1002/2014GL060509.
Wendling, V., Peugeot, C., Mayor, A.G., Hiernaux, P., Mougin, E., Grippa, M., Kergoat, L., Walcker, R., Galle, S., Lebel, T., 2019. Drought-induced regime shift and resilience of a Sahelian ecohydrosystem. Environ. Res. Lett. 14, 105005 https://doi.org/10.1088/1748-9326/ab3dde.
Yonaba, R., Biaou, A.C., Koïta, M., Tazen, F., Mounirou, L.A., Zouré, C.O., Queloz, P., Karambiri, H., Yacouba, H., 2021. A dynamic land use/land cover input helps in picturing the Sahelian paradox: assessing variability and attribution of changes in surface runoff in a Sahelian watershed. Sci. Total Environ. 757, 143792 https://doi.org/10.1016/j.scitotenv.2020.143792.
Zhang, L., Walker, G.R., Dawes, W., 1999. Predicting the effect of vegetation changes on catchment average water balance. Coop. Res. Cent. Catchment Hydrol. CSIRO Land Water.
Zhang, L., Dawes, W., Walker, G., 2001. Response of mean annual evapotranspiration to vegetation changes at catchment scale. Water Resour. Res. 37, 701–708.
Zhang, L., Hickel, K., Dawes, W., Chiew, F.H., Western, A., Briggs, P., 2004. A rational function approach for estimating mean annual evapotranspiration. Water Resour. Res. 40 https://doi.org/10.1029/2003WR002710.
Zhang, H., Xu, W., Xu, X., Lu, B., 2017. Responses of streamflow to climate change and human activities in a River Basin, Northeast China. Adv. Meteorol. 2017, 10. https://doi.org/10.1155/2017/1023821.
Zhang, Xiao-feng, Yan, H., Yue, Y., Xu, Q., 2019. Quantifying natural and anthropogenic impacts on runoff and sediment load: an investigation on the middle and lower reaches of the Jinsha River Basin. J. Hydrol. Reg. Stud. 25, 100617 https://doi.org/10.1016/j.ejrh.2019.100617.
Zhang, Xu, Dong, Q., Cheng, L., Xia, J., 2019a. A Budyko-based framework for quantifying the impacts of aridity index and other factors on annual runoff. J. Hydrol. 579, 124224 https://doi.org/10.1016/j.jhydrol.2019.124224.
Zhang, Xu, Dong, Q., Costa, V., Wang, X., 2019b. A hierarchical Bayesian model for decomposing the impacts of human activities and climate change on water resources in China. Sci. Total Environ. 665, 836–847. https://doi.org/10.1016/j.scitotenv.2019.02.189.
Zhu, S., Xu, Z., Luo, X., Wang, C., Zhang, H., 2019. Quantifying the contributions of climate change and human activities to drought extremes, using an improved evaluation framework. Water Resour. Manag. 33, 5051–5065. https://doi.org/10.1007/s11269-019-02413-6.
Zouré, C., Queloz, P., Koita, M., Niang, D., Fowé, T., Yonaba, R., Consuegra, D., Yacouba, H., Karambiri, H., 2019. Modelling the water balance on farming practices at plot scale: case study of Tougou watershed in Northern Burkina Faso. Catena 173, 59–70. https://doi.org/10.1016/j.catena.2018.10.002.
Zuo, D., Xu, Z., Wu, W., Zhao, J., Zhao, F., 2014. Identification of streamflow response to climate change and human activities in the Wei River Basin, China. Water Resour. Manage. 28, 833–851. https://doi.org/10.1007/s11269-014-0519-0.